國立臺灣大學醫學院臨床醫學研究所

博士論文

Graduate Institute of Clinical Medicine

College of Medicine

National Taiwan University

Doctoral Dissertation

新興膽管癌藥物研究

Novel Target Signaling Pathway for the Treatment of Cholangiocarcinoma

胡名宏

Ming-Hung Hu

指導教授：高嘉宏 教授 劉俊人 教授

Advisor: Jia-Horng Kao MD,Ph.D Chun-Jen Liu MD,Ph.D

中華民國 一百一十三 年 七 月

July, 2024

doi:10.6342/NTU202404281

ACKNOWLEDGEMENT

This work was conducted at the Graduate Institute of Clinical Medicine, National Taiwan University, between 2014 and 2018.

My days at the Graduate Institute of Clinical Medicine fulfilled my dream of becoming a physician-scientist. It was a unique and exhausting, yet rewarding journey, balancing my roles as a cancer physician and PhD student simultaneously. I am deeply grateful to all the people who provided me with tremendous support along the way.

First, I would like to thank Prof. Jia-Horng Kao, Prof. Chun-Jen Liu, and Dr. Kuen-Feng Chen, who have been exceptional mentors and have guided me throughout my PhD journey. They have continuously provided me with both the hard and soft skills necessary for conducting basic research. I would also like to express my gratitude to my other supervisors, Dr. Chun-Yu Liu and Dr. Ming-Huang Chen from Taipei Veterans General Hospital, who sparked my interest in cancer research and have been invaluable mentors. In addition, I would like to thank all my teachers and professors at the Graduate Institute of Clinical Medicine, who have taught and trained me to become a successful scholar. Special mention goes to Li-Ju Chen, Ming-Shen Tsai, Dr. Tzu-I Chao, Dr. Yen-Lin Chen, and Dr. Tung-Hung Su for their outstanding collaboration in the laboratory and their generous technical support.

I warmly acknowledge the members of my thesis committee Prof. Li-Tzong Chen, Prof. Chun-Yen Lin and Prof. Hung-Chih Yang, for being an active part of the process and offering valuable suggestions for improvements. Their reviewing comments deserve a thousand thanks for thorough and prompt work. Their constructive and encouraging comments and discussions were very helpful in finalizing the thesis. Last but not least, I am deeply grateful to my family, particularly my parents, parents-in-law, my wife, and my two little girls. I am thankful for the unwavering encouragement and support from my parents and parents-in-law. To my wife, I-Ping Hsu, whose

doi:10.6342/NTU202404281

understanding and support during my time away from family life were invaluable. I also want to acknowledge my little girls for bringing immense joy and happiness into my life, providing meaning beyond work and academics.

Ming-Hung Hu

doi:10.6342/NTU202404281

CHINESE ABSTRACT 中文摘要

膽管癌是一種高惡性度之侵襲性癌症，由於缺乏明顯症狀、診斷不易以及有限的藥物治療選擇，造成膽管癌病人預後不佳，治療上帶來相當大的臨床挑戰。由於目前標準治療的療效不盡理想，開發新型膽管癌的治療藥物無疑成為一項重要使命。蛋白激脢是調節多種重要細胞功能如細胞增殖及細胞代謝的酵素，並且在發炎反應中扮演關鍵角色，而膽管細胞的發炎反應是導致各種膽管癌亞型的主要風險，包括膽管癌在內的發炎性癌細胞中，signal transducers and activators of transcription 3 (STAT3)等激脢常常被過度活化，而蛋白激脢的活性及其上下游相關的激脢均會受到磷酸脢的負向調節，這些磷酸脢負責激脢的去磷酸化，與激脢的活性息息相關。與蛋白激脢相同，磷酸脢在調節細胞細胞活動中也扮演著重要的角色對於多種細胞的功能至關重要。Serine/ threonine protein phosphatase 5 (PP5)，屬於磷蛋白磷酸脢 (PPP)家族當中，一種參與調節壓力信號和細胞增長的獨特磷酸脢。我們的研究專注於抑制蛋白激脢或抑制磷酸脢的調控，藉以開發新型膽管癌治療藥物。在我們的兩個概念驗證模型當中，展示了開發膽管癌新型治療劑的潛在機制。第一個模型顯示，藉由新型Sorafenib衍生物調控 SHP-1，抑制磷酸化的 STAT3 可以作為潛在的治療策略。第二個模型則發現，通過調控 AMPK 來抑制 PP5，亦是一種可能的膽管癌治療途徑。我們衷心地希望透過這些發現，能為未來膽管癌的治療藥物的研發盡上一份微薄貢獻。

關鍵字: 膽管癌、STAT3、SHP-1、PP5、AMPK

doi:10.6342/NTU202404281

ENGLISH ABSTRACT

Cholangiocarcinoma (CCA) is an aggressive disease with a dismal prognosis due to its silent presentation, delayed diagnosis, and limited effective treatment options. The significant unmet medical need in patients with CCA presents a substantial clinical challenge. Due to the unsatisfactory therapeutic outcomes associated with the current standard treatments, the development of novel agents for CCA treatment is undeniably an essential mission. Protein kinases, enzymes that regulate numerous essential cellular functions such as proliferation and cell metabolism, play a key role in inflammation, which represents the main risk factor shared by all CCA subtypes. Kinases such as signal transducers and activators of transcription 3 (STAT3) are frequently activated in inflammatory cancer cells including CCA. The activities of protein kinases and their upstream or down-stream kinases are negatively regulated by protein phosphatase, which are responsible for the dephosphorylation of these kinases. Similar to kinases, protein phosphatases play a fundamental role in regulating cellular activities, as protein phosphorylation and dephosphorylation are essential for a wide range of cellular functions. Serine/threonine protein phosphatase 5 (PP5), belong to the phosphoprotein phosphatase (PPP) family, is a unique phosphatase that participate in regulating stress signaling and cell growth. We focus on discovering new agents for CCA treatment not only regulating kinase but also phosphatase pathway. We focus on discovering new agents for CCA treatment through the inhibition of not only kinase but also phosphatase pathways. Our two proof-of-concept models demonstrate the potential mechanisms for developing novel therapeutic agents for CCA. The first model demonstrates that inhibiting phosphorylated STAT3 by a novel Sorafenib derivative, through the regulation of SHP-1, is a potential therapeutic strategy. The second model, on the other hand, suggests that targeting PP5A through the regulation of AMPK presents an appealing treatment pathway for CCA. We hope that our findings will pave the way for the development of new treatments for CCA in the future.

doi:10.6342/NTU202404281

Keywords: Cholangiocarcinoma, STAT3, SHP-1, PP5, AMPK

doi:10.6342/NTU202404281

目　次

doi:10.6342/NTU202404281

圖　次

doi:10.6342/NTU202404281

doi:10.6342/NTU202404281

1.INTRODUCTION

My research interests focus on the management of solid cancers and hematological cancers, especially novel treatment development. As a medical oncologist and hematologist, I realize that drug innovation is fundamental for the management of patients with late-stage cancer disease. Cholangiocarcinoma (CCA) is one of the most aggressive cancer types with extremely poor prognosis. In this thesis, two different proof-of-concept models are provided to support the both direct and indirect pathway interact with phosphatase can be a novel treatment strategy for CCA. The first model showcases that targeting phosphorylated STAT3 by enhancing SHP-1 activity provide therapeutic effect for CCA, especially inflammatory-related CCA. The second model demonstrates that inhibiting PP5 activity with AMPK upregulation might be a potential treatment pathway.

1.1 Unmet medical need in CCA

CCA is a fetal hepatic malignancy, which is second most common after hepatocellular carcinoma (HCC).[1,2] CCAs belongs to epithelial malignancies that arise from cholangiocytes and are characterized by aggressive behavior and advanced clinical stage. Although CCA is not a common malignancy, account 3% of all gastrointestinal cancers, the overall incidence of CCA has increased significantly over the past three decades.[3,4] Meanwhile, the mortality from CCA is still increasing.[5] Until recently, several targeted agents and immunotherapies have been approved for the treatment of CCA.[4,6-10] In addition to targeting therapy, cytotoxic chemotherapy remains main choice for unresectable metastatic CCA. However, 5-year survival rate of CCA is extremely poor, remaining at 10%.[11,12] The unmet medical need in patients with CCA remains a great clinical challenge. Owing to the unsatisfactory therapeutic outcomes under the current standard management, development of novel agents for treatment of CCA is undoubtedly an important mission.

1.2 The role STAT3 in the pathogenesis of CCA

Given the evidence of endemic infection in the development of CCA, chronic inflammation marked by the presence of specific inflammatory cells and inflammatory cytokines play a key role in

doi:10.6342/NTU202404281

CCA.[2,13-15] Signal transducers and activators of transcription 3 (STAT3) belong to a family of transcription factors that relay cytokine receptor-generated signals into the nucleus. Regulation of STAT3 relies on the cytokine IL-6 as well as numerous growth factors, including epidermal growth factor receptor (EGFR), fibroblast growth factor receptor (FGFR), and platelet-derived growth factor receptor (PDGFR) through tyrosine phosphorylation.[16] After activation, dimerized STAT3 translocates into the nucleus where it activates gene transcription. STAT3 signaling mediates cell growth, proliferation, inflammatory cytokine production, cell invasion and migration. Chronic stimuli such as *O.viverrini* infection or primary sclerosing cholangitis cause persistent inflammation and cholestasis of the bile duct, leading to a variety of cytokines production including IL-6, platelet-derived growth factor (PDGF), and epidermal growth factor (EGF).[17-19] This inflammatory cascade activates STAT3, leading to overproduction of bile duct epithelium growth factor, thus promoting CCA initiation. Because of the role of STAT3 in inflammation and cancer development, targeting STAT3 is a rational treatment strategy for CCA.[20,21]

1.4 STAT3 is a potential targeting pathway in CCA treatment

STAT3 is traditionally regarded as an undruggable target due to its transcription factor characteristics. Current STAT3-targeting compound could be divided into indirect and direct inhibitors.[22] Indirect inhibitors target the upstream signals of the STAT3 pathway that inhibit STAT3 phosphorylation. For instance, roxulitinib, a JAK inhibitor, can reduce STAT3-related inflammation and is approved for the use in myelofibrosis.[23] Dasatinib, an SRC kinase inhibitor approved for the treatment in chronic myeloid leukemia, can induce STAT3-dependent cancer cell apoptosis.[24] Direct STAT3 inhibitor, in the other hand, is under rapid development because of excellent physicochemical and limited toxicity properties. Current research of direct inhibitors focuses on SH2 and SHP-1, given its critical role in STAT3 regulation. C188-9 (TTI-101) was developed for the treatment of advance tumors and was currently evaluated in phase I clinical study of liver cancer and head-and-neck cancer.[25,26] In addition, preclinical data shows that C188-9 can reverse the progression of

doi:10.6342/NTU202404281

nonalcoholic steatohepatitis (NASH),[27] which is a well-known risk of CCA. Therefore, we hypothesized that STAT3 inhibition could be a potential therapeutic agent for CCA by its SHP-1-regulated STAT3 inhibition.

1.5 Sorafenib derivative act as a STAT3 inhibitor and potential therapeutic agent for CCA

Sorafenib acts as a multiple kinase inhibitor that works against rapidly accelerated fibrosarcoma (Raf) kinases, vascular endothelial growth factor receptor (VEGFR), and PDGFR, among others. Boris et al. revealed that sorefenib inhibits CCA cells by downregulating STAT3 signaling [28]. Previously, we discovered that SHP-1, a nonreceptor protein tyrosine phosphatase (PTP) that negatively regulates p-STAT3, is also a direct target of sorafenib [29,30]. Accordingly, we have synthesized a series of sorafenib analogs which resemble sorafenib structure closely but have no kinase inhibition activities. Among these derivatives, SC-43 was found to be a more potent SHP-1 agonist than sorafenib. Our earlier study demonstrated that SC-43 had therapeutic potential in HCC treatment [29]. Based on this preclinical success, SC-43 is currently poised to enter a phase I clinical trial for treatment of HCC.

1.6 Diverse functional phosphatase with unknown role for cancer treatment

Protein phosphorylation plays a key role in controlling a variety of cellular processes, such as migration, proliferation, apoptosis, differentiation, metabolism, organelle trafficking, immunity, learning and memory.[31,32] Reversible phosphorylation catalyzed by protein kinases and phosphatases has been shown to play an important role in the regulation of numerous signaling networks. The main role of phosphatase is to regulate post-translational protein function, leading to cellular signaling function modification. Alternation of phosphatase activity is a hallmark of cancer cell resistance,[33] while numerous phosphatases appear to have close interaction with CCA.[34-36] Novel agent targeting on protein kinase has developed as a major field for cancer drug innovation, however, whether phosphatase could be used for cancer treatment is widely unknown.

1.7 The role of serine/threonine protein phosphatase 5 in CCA is undetermined

doi:10.6342/NTU202404281

Unlike SHP-1, serine/threonine protein phosphatase 5 (PP5) and other serine/threonine protein phosphatases such as PP1, PP2A, and PP2B belong to the phosphoprotein phosphatase (PPP) family. PP5 is unique among the PPP family because of its low basal activity caused by its autoinhibitory N-terminal tetratricopeptide (TPR) domain.[37,38] It has been suggested that PP5 may participate in regulating stress signaling and cell growth,[39] as overexpression of PP5 in MCF-7 breast cancer cells enabled profound MCF-7 proliferation in estrogen-deprived culture media.[40] One of the most studied functions of PP5 is the regulation of hormone- and stress-induced cellular signaling through the glucocorticoid receptor (GR)-heat shock protein 90 (Hsp-90) complex [41]. In addition, PP5 negatively regulates several signaling pathways, such as the Raf-1/ERK [42] and apoptosis signal regulating kinase (ASK1)/MKK4/JNK pathway [43]. Furthermore, PP5 appears to function as a negative regulator of the p53-tumor suppressor protein [44]. Recently, aberrant expression of PP5 has been reported in several malignancies. Overexpression of PP5 in MCF-7 breast cancer cells enabled profound cell proliferation [40]. In contrast, knockdown of PP5 repressed colony formation and cell proliferation in glioma, hepatocellular carcinoma, and ovarian cancer cell lines [45-47]. Given that PP5 appears to regulate proliferation in malignant cells, its role in CCA and its potential as a pharmacotherapeutic target merits further investigation.

1.8 PP5 inhibitor is a potential therapeutic anti-cancer agent

Mammalian PP5 has been identified to be sensitive to several natural toxins. Cantharidin (CTD), an active ingredient extracted from the defensive toxin of blister beetles, has been recognized as a potent inhibitor of PPPs [48,49]. Norcantharidin (NCTD) is a demethylated analog of CTD [50]. Both NCTD and CTD have anticancer activities [50,51]. However, the use of CTD in animal experiments is not feasible because of its significant gastrointestinal and urinary toxicity [52]. Compared with CTD, NCTD causes fewer adverse inflammatory effects [50,52] and attracts more interest for its clinical application. Therefore, we assumed that NCTD might provide a better therapeutic effect in the treatment of CCA.

doi:10.6342/NTU202404281

Owing to the pivotal function of different phosphatase SHP-1 and PP5 in CCA, the potential role of its targeting value should be further evaluated. In our study, we hypothesize that SC43 might have antitumor effect in CCA though SHP-1-regulated STAT3 inhibition. Furthermore, whether PP5 is a druggable signaling in CCA would be tested. In this present study, we will assess the effect of SC-43 and CTD on CCA cells, in order to investigate the underlying molecular mechanism.

doi:10.6342/NTU202404281

2. MATERIAL AND METHODS

2.1 Material and methods in targeting SHP-1-STAT3 study

Reagents and antibodies

SC-43 was dissolved in dimethyl sulfoxide and then added to the cells maintained in RPMI 1640 medium without FBS. SHP-1 inhibitor (PTPIII) was purchased from Calbiochem. Antibodies, such as cyclin D1, STAT3, phospho-STAT3 (Tyr705), survivin, and caspase-9 were purchased from Cell Signaling (Danvers, MA). Other antibodies, such as cyclin B1 and Cdc2 were purchased from Abcam (London).

Cell culture and western blot analysis

The HuCCT-1 cell line was purchased from Riken BRC (Riken BioResource Center) (Saitama, Japan). The KKU-100 cell line was obtained from JCRB Cell Bank (Japanese Collection of Research Bioresources Cell Bank) (Osaka, Japan). The CGCCA cell line was kindly provided by Taipei Veterans General Hospital. HuCCT-1 cells was routinely cultured in RPMI 1640 (Invitrogen/Life Technologies, Saint Aubin, France), while KKU-100 and CGCCA cells were cultured in Dulbecco's modified Eagle's medium (Gibco/Life Technologies, Grand Island, NY). All CCA cells were supplemented with 10% heat-inactivated fetal bovine serum (Gibco/Life Technologies, Grand Island, NY), 100 μg/mL streptomycin sulfate, and 100 μg/mL penicillin, in a humidified atmosphere containing 5% CO_2 at 37°C. Lysates of CCA cells treated with drugs at the indicated concentrations for various periods of time were prepared for immunoblotting of p-STAT3, STAT3, etc. Whole-cell lysates were resolved by sodium dodecyl sulfate polyacrylamide gel electrophoresis. Proteins were transferred onto a polyvinylidene difluoride membrane (Millipore, Billerica, MA) and incubated with the primary antibody, and then incubated with horseradish peroxidase–conjugated secondary antibodies. Specific proteins were detected using enhanced chemiluminescence reagent.

doi:10.6342/NTU202404281

Cell viability and proliferation of CCA cell lines in vitro

Cell viability and proliferation of CCA cells treated with or without SC-43 were assessed by colorimetric assay using 3-(4,5-dimethylthiazol-2-yl)-2,5 diphenyltetrazolium bromide (MTT). Cells were plated in a 96-well plate in 100 μl DMEM per well and cultured for up to 72 hours. Cells were incubated for four hours at 37°C with MTT; after incubation, medium was removed and cells were treated with dimethyl sulfoxide (DMSO) for five minutes. Viability was evaluated by ultraviolet absorption spectrum at 540 nm with a Microplate Reader Model 550 (Bio-Rad, Richmond, CA, USA). Experiments were performed three times in duplicate.

Apoptosis analysis

Drug-induced apoptotic cell death was assessed by measuring apoptotic cells by flow cytometry (sub-G1 analysis of propidium iodide-stained cells) and western blot analysis of caspase 3 cleavage.

Generation of CCA cells with ectopically expressed STAT3

STAT3 cDNA (KIAA1524) were purchased from Addgene plasmid repository (http://www.addgene.org/). HuCCT-1 cells with ectopic expression of STAT3 derived from a single-stable clone were prepared for in vitro assay for STAT3 target validation. Briefly, HuCCT-1 was incubated in the presence of G418 (0.78 mg/ml). After 8 weeks of selection, surviving colonies, i.e., those arising from stably transfected cells, were selected and individually amplified. Control cells were transfected by empty vectors.

Gene Knockdown Using siRNA

Smart-pool siRNAs, including control (D-001810-10), SHP-1 (PTPN6, L-009778- 00-0005), and STAT3 were all purchased from Dharmacon (Chicago, IL). Plasmids of human wild-type STAT3 and SHP-1 (PTPN6) were encoded by pCMV6 vector with myc-tag. For mutant-type SHP-1

doi:10.6342/NTU202404281

expression, we generated two plasmids, designated dN1 and D61A, with a truncated N-SH2/PTP domain and aspartic acid at 61 changed to an alanine residue, respectively. Both plasmids were cloned into pCMV6 entry vector. These plasmids or siRNAs were subsequently transfected into cells by using Lipofectamine 2000 Reagent (Invitrogen, CA).

SHP-1 phosphatase activity assay

After treatment of SC-43, the cellular protein extracts were incubated with anti-SHP-1 antibody in immunoprecipitation buffer (20 mM of Tris-HCl [pH 7.5], 150 mM of NaCl, 1 mM of ethylenediaminetetraacetic acid, 1% NP-40, and 1% sodium deoxycholate) overnight. Protein G-Sepharose 4 Fast flow (GE Healthcare Bio-Science, NJ) was added to each sample, followed by incubation for 3 hours at 4°C with rotation. A RediPlate 96 EnzChekR Tyrosine Phosphatase Assay Kit (R-22067) was used for SHP-1 activity assay (Molecular Probes, Invitrogen, CA).

Xenograft tumor growth

Male NCr athymic nude mice (5-7 weeks of age) were obtained from the National Laboratory Animal Center (Taipei, Taiwan, ROC). The mice were housed in groups and maintained in an SPF-environment. All experimental procedures using these mice were performed in accordance with protocols approved by the Institutional Animal Care and Use Committee of Cardinal Tien Hospital. Each mouse was inoculated orthotopically to the mouse mammary pads with 5×10^6 HuCCT-1 cells suspended in 0.1 mL serum-free medium containing 50% Matrigel (BD Biosciences, Bedford, MA) under isoflurane anesthesia. Tumors were measured using calipers and their volumes calculated using a standard formula: $\text{width}^2 \times \text{length} \times 0.52$. When tumors reached around 100 mm^3, mice were administered orally with SC-43 at 10 mg/kg or 30 mg/kg daily by oral gavage. Controls received vehicle (1× phosphate buffered saline). Upon termination of treatment, mice were sacrificed and xenografted tumors were harvested and assayed for tumor weight, SHP-1 activity, and molecular

doi:10.6342/NTU202404281

events by western blot analysis.

Immunohistochemistry

Immunohistochemical (IHC) stains were performed, using the Ventana BenchMark XT automated stainer (Ventana, Tucson, AZ). Briefly speaking, 4-μm thick sections would be cut consecutively from formalin-fixed, paraffin-embedded (FFPE) human tissue. Sections would be mounted and allowed to dry overnight at 37°C. After deparaffinization and rehydration, slides would be incubated with 3% hydrogen peroxide solution for 5 minutes. After a washing procedure with the supplied buffer, tissue sections were repaired for 40 minutes with ethylenediamine tetra-acetic acid. The slides were then incubated with primary antibodies against p-STAT3 (1:50; Cell Signaling) for 60 minutes at 37°C and overnight at 4˚C. Negative control slides processed without the primary antibody were included for each staining. After three rinses in buffer, the slides were incubated with the secondary antibodies (unbiotinylated antibody; EnVisionTM System; HRP, anti-mouse/rabbit, DakoCytomation; Dako, Glostrup, Denmark). Tissue staining were visualized with a 3,3′-diaminobenzidine (DAB) substrate chromogen solution (DakoCytomation). Slides were counterstained with hematoxylin, dehydrated, and mounted. Samples which express these markers strongly served as the positive controls. The mean percentage of positive tumor cells was determined in at least five areas at x200 magnification. All slides were evaluated by experienced pathologists who reviewed the slides together and reached a consensus. Positive expression for p-STAT3 was defined as >25% nuclear staining with greater than moderate staining intensity of tumor cells.

Statistical analysis

All data are expressed as mean ± SD or SE. Statistical comparisons were based on nonparametric tests. P value less than 0.05 was defined as statistical significance. All statistical analyses were performed using SPSS for Windows software, version 19.0 (SPSS, Chicago, IL, USA).

doi:10.6342/NTU202404281

2.2 Material and methods in targeting PP5 study

Chemicals, plasmid constructs, and antibodies

CTD and the AMPK inhibitor (dorsomorphin dihydrochloride; compound C) were purchased from MedchemExpress (NJ, USA). CTD was obtained from Sigma-Aldrich (MO, USA). For the *in vitro* studies, CTD was dissolved in dimethyl sulfoxide at the designated concentrations and added to serum-free Dulbecco's modified Eagle's medium (DMEM) or serum-free RPMI 1640 medium. For the *in vivo* experiments, NCTD was dissolved in ddH_2O and orally administered at a dosage of 40 mg/kg/day. Antibodies against β-actin (Sigma-Aldrich, MO, USA), PP5, PARP, (Santa Cruz Biotechnology, CA, USA), AMPK, p-AMPK (Thr172), ACC, p-ACC, caspase-9**,** p-ASK1 (Thr845), ASK1, p-JNK(Thr183/Tyr185), JNK, cyclin D1(Cell Signaling Technology, MA, USA), and DDK (OriGene, MD, USA) were purchased from the commercial suppliers indicated above. The PP5 activator (arachidonic acid; AA) was purchased from BioVision (CA, USA). Human PP5 cDNA was subcloned into the pCMV-Tag2B vector (Agilent Technologies, CA, USA) to express DDK-PP5. ON-TARGETplus human AMPKα2 (PRKAA2) siRNA was purchased from GE Dharmacon (CO, USA). The bromodeoxyuridine (BrdU) cell proliferation kit (K306) was purchased from BioVision (Milpitas, CA, USA).

Cell culture and transfection

The human CCA cell line HuCCT1, which was derived from human intrahepatic CCA [53], was purchased from Riken BioResource Center (Saitama, Japan). KKU100, the first *Opisthorchis viverrini* (*O. viverrini*)-associated hilar CCA cell line [54], was purchased from the Japanese Collection of Research Bioresources Cell Bank (Osaka, Japan). The CGCCA cell line was derived from an oral thioacetamide (TAA)-induced model of rat CCA and has been widely used as a preclinical platform for therapeutic investigation in human CCA [55,56]. The CGCCA cells were a generous gift from Taipei

doi:10.6342/NTU202404281

Veterans General Hospital. CCA cells were cultured in DMEM or RPMI 1640 medium supplemented with 10% fetal bovine serum (Gibco). Cells were maintained at 37°C with 5% CO_2 in a humidified incubator. Recombinant lentiviruses were used to establish ectopic expression or knockdown cell lines. The lentiviral transfer vector pLAS2w.Ppuro carrying DDK-PP5 was used to generate PP5-overexpressing cell pools. To establish stable PP5-knockdown cell pools, pLKO.1-puro vectors expressing either shRNAs targeting PP5 (TRCN0000002801 & TRCN0000002802) or control shRNA (pLKO TRC025) were used. The two different PP5 shRNA sequences were as follows:

shPP5#1

(5′CCGGCCACGAGACAGACAACATGAACTCGAGTTCATGTTGTCTGTCTCGTGGTTTTT3′) and

shPP5#2

(5′CCGGGAGACAGAGAAGATTACAGTACTCGAGTACTGTAATCTTCTCTGTCTCTTTTT3′).

The recombinant lentiviruses, as well as the shRNA reagents, were purchased from the National Core Facility for Manipulation of Gene Function by RNAi (Academia Sinica, Taiwan). The transfection procedure was in accordance with the instructions in the manufacturer's protocol. Briefly, CCA cells were transfected with shRNA in 6-well plates with fresh transfection media. After incubation for 24 hours, puromycin was added to the CCA cells for selection, and the cells were incubated for an additional 48 hours.

Western blot analysis

Lysates of CCA cells treated with drugs at the indicated concentrations for various periods of time were prepared for immunoblotting of p-AMPK, AMPK, etc. Whole-cell lysates were resolved by sodium dodecyl sulfate polyacrylamide gel electrophoresis. Proteins were transferred onto a polyvinylidene difluoride membrane (Millipore, Billerica, MA) and incubated with the appropriate

doi:10.6342/NTU202404281

primary antibody and then incubated with horseradish peroxidase–conjugated secondary antibodies. Specific proteins were detected using enhanced chemiluminescence reagent. The signals were visualized by exposing the membranes to X-ray films. The quantitation of the resulting bands was calculated as OD × band area by a one-dimensional (1-D) image analysis system.

Colony formation assay

Cells were cultured at a density of 500 cells per well in 6-well plates for 14 days. Then, the colonies were fixed and stained with 0.5% crystal violet before being analyzed using an inverted microscope.

Tumorsphere formation assay

Cells were plated at a density of 100 cells per well in an ultra-low attachment dish (Corning) for 14 days and the numbers of tumorspheres formed were calculated.

PP5 activity measurement

The human CCA cells were treated with CTD at the indicated concentrations for 24 hours. Next, cells were collected and immunoprecipitated with antibodies against PP5 (SC-271816, Santa Cruz Biotechnology, Santa Cruz, CA). PP5 activity was measured by using the RediPlate 96 EnzChek Serine/Threonine Phosphatase Assay Kit (Thermo Fisher). For PP5 activity analysis in a cell-free system, HuCCT1 cells were first immunoprecipitated with antibodies against PP5 (Santa Cruz Biotechnology). The immunoprecipitant was then incubated with CTD at room temperature for 30 minutes. Finally, the RediPlate 96 EnzChek Serine/Threonine Phosphatase Assay Kit (Thermo Fisher) was employed to measure PP5 activity.

Bromodeoxyuridine cell proliferation assay

doi:10.6342/NTU202404281

The evaluation of cell proliferation was performed with a BrdU kit according to the manufacturer's protocol. In the BrdU cell proliferation assay, BrdU, a pyrimidine analog, is incorporated instead of thymidine into replicating DNA, and then immunodetection of BrdU using specific monoclonal antibodies allows cells in the S phase of the cell cycle to be labeled. CCA cells were treated with different concentrations of CTD. BrdU solution was added to the desired wells and the plates were incubated at 37°C for 4 hours. After removal of the BrdU labeling solution, the kit's fixing/denaturing solution was applied for 30 minutes at room temperature to fix and denature the cells. Then, the cells were incubated for 1 hour with BrdU detection antibody solution. After washing off the unbound anti-BrdU-POD, anti-mouse HRP-linked antibody solution was added. Furthermore, TMB substrate solution was added into each well. Color development was monitored and measured at an absorbance of 650 nm.

Animal models and experiments

The animal experiment protocols were approved by the Institutional Animal Care and Use Committee of National Taiwan University. Male NCr athymic nude mice (5 weeks of age) were purchased from the National Laboratory Animal Center (Taipei, Taiwan). For the HuCCT1 PP5 knockdown xenograft model, mice (n=5) were subcutaneously inoculated in the dorsal flank with 5×10^6 lentiviral-transduced PP5-knockdown HuCCT1 cells (HuCCT1 shPP5#1 or HuCCT1 shPP5#2) or control (HuCCT1 shControl) cells with 50% Matrigel (BD Biosciences, Bedford, MA). To facilitate the PP5 knockdown xenograft engraftment rate, we selected the higher dose of 5×10^6 rather than 2×10^6 cells. For the CTD treatment experiment, 2×10^6 HuCCT1 cells were suspended in serum-free medium with 50% Matrigel (BD Biosciences, Bedford, MA). The cells were then inoculated subcutaneously. The tumor sizes were measured twice weekly, in a blinded manner, using calipers. The tumor sizes were approximated by using the following formula: $\text{width}^2 \times \text{length} \times 0.52$.

doi:10.6342/NTU202404281

Cancer Genome Atlas data description

PPP5C expression data from normal tissue (*n*=9) and CCA samples (*n*=36) were downloaded from The Cancer Genome Atlas (TCGA) (https://tcga-data.nci.nih.gov/tcga/). Data processing and quality control were conducted with the Broad GDAC Firehose data portal (https://gdac.broadinstitute.org/). The mRNA reads per expectation maximization (RSEM) of all samples was analyzed with GraphPad Prism software.

Statistical analysis

Statistical analyses were performed using GraphPad Prism (version 6, GraphPad Software Inc.). A *p* value of less than 0.05 was considered to be statistically significant.

doi:10.6342/NTU202404281

3. RESULTS

3.1 Results in targeting SHP-1-STAT3 study

Novel sorafenib derivative SC-43 induced apoptosis in CCA cells by inducing G_2-M arrest

In CCA cells from representative tumor tissue from a CCA patient, p-STAT3 showed positive expression in the tumor part (Fig 1-A, left) compared with normal tissue part (Fig 1-A, right). SC-43 is a novel derivative of sorafenib. To investigate the apoptosis effect induced by SC-43, we tested three CCA cell lines: HuCCT-1, KKU-100, and CGCCA. First, as shown in Fig 1-B, MTT assay revealed the anti-proliferative effects of SC-43 in CCA cell lines in a dose-dependent manner after treating 24, 48 and 72 hours respectively. Next, flow cytometry analysis showed increased sub-G1 cells and G_2-M arrest, indicating SC-43 induced differential apoptotic effects in these cell lines, which corresponds with the MTT assay (Fig 2-A). In addition, CCA cells treated with SC-43 demonstrated significant increase in cleaved caspase-3 and PARP level in western blot analysis after exposure for 24 hours (Fig 2-B). Taken together, these data indicated that SC-43 has a significant effect to induce G_2-M arrest on CCA cell, leading to apoptosis and growth inhibition.

SC-43 induces apoptosis with downregulation of STAT3 in CCA cells

Next, we examined whether STAT3 had a relationship with SC-43-induced apoptosis in CCA cells. In Fig 3-A, SC-43 was demonstrated to dose-dependently downregulate p-STAT3 and its downstream mediators, survivin and cyclin D-1. STAT 3 level did not diminish after SC-43 treatment. Furthermore, SC-43-induced downregulation of the p-STAT3 signaling pathway in KKU-100 was time-dependent (Fig 3-B), as well as in HuCCT-1 and CGCCA (Fig 4). In STAT3 overexpressing CCA cells, inhibition of p-STAT3 after SC-43 treatment was reduced. The apoptosis in STAT3 overexpressing cancer cells was reversed as well (Fig 5-A). We further explored the role of SC-43 involving G_2-M arrest. We performed western blot analysis of cell extracts to compare the levels of expression of the cyclin B1 and Cdk1 (Cdc2), the major regulatory protein and kinase for progression

doi:10.6342/NTU202404281

from G_2 to M phase. Western blotting demonstrated that the levels of the cyclin B1 and Cdc2 protein were markedly reduced after SC-43 treatment (Fig 5-B). In summary, we hypothesized that SC-43 had an antiproliferative effect on CCA cells through inhibiting the STAT3 pathway, as well as G_2-M arrest by inhibiting cyclin B1 and Cdc2

Validation of the SHP-1/p-STAT3 pathway as a molecular determinant of SC-43 induced CCA cell apoptosis

In this study, we assumed that SHP-1 may also play a role in the biological reaction associated with apoptosis induced by SC-43 in CCA cells. First, we tested SHP-1 phosphatase activity in the above three CCA cell lines: HuCCT-1, KKU-100, and CGCCA. As illustrated in Fig 6-A, SHP-1 activity was universally increased in all cell lines after SC-43 treatment. Furthermore, SC-43 increased the phosphatase activity of SHP-1 in IP-SHP-1 cell lysate from HuCCT-1 cells, suggesting that SC-43 activates SHP-1 through direct interaction with SHP-1 proteins (Fig 6-B). To validate the role of SHP-1 in mediating SC-43-induced apoptosis, we utilized PTPIII, a SHP-1 specific inhibitor. The protective effects of SC-43-induced apoptosis in HuCCT-1 and KKU-100 cells were noted after PTPIII administration (Fig 6-C). After HuCCT-1 cells were transfected with SHP-1 siRNA, SC-43-induced apoptosis was reduced significantly in SHP-1-silencing HuCCT-1 cells, comparing to cells transfected with control si-RNA (Fig 7, left). Then, we generated HuCCT-1 cells with constitutive, ectopic expression of myc-tagged SHP-1. SC-43 treatment in HuCCT-1 with high levels of SHP-1 showed more inhibition of p-STAT3 and more cell apoptosis, compared to cells transfected with empty vectors (Fig 7, right). Taken together, these results suggested that SC-43 mediates the apoptotic effect in CCA cells through p-STAT3 inhibition by activating SHP-1 activity.

SC-43 relieves autoinhibition of SHP-1 by interfering with the inhibitory N-SH2 domain

As the activity of SHP-1 was strongly regulated by the auto-inhibited 3D structure, we

doi:10.6342/NTU202404281

constructed wild-type, deletion of N-SH2 (dN1), and D61 single mutant (D61A) of SHP-1 to investigate the effect of SC-43 on different SHP-1 statuses (Fig. 8A). The dN1 and D61A mutants resemble open (non-autoinhibition) forms. As demonstrated in Fig. 8B, SC-43 induced significantly less p-STAT3 downregulation and apoptosis in HuCCT-1 cells expressing the dN1 and D61A mutants than in the wild-type control, suggesting that N-SH2 and PTPase catalytic domain are important for SC-43 induced effects. The conformational change of SHP-1 induced by dN1 and D61A counteracted the SC-43 effect. Furthermore, dose-escalation study of transfection of dN1 and D61A suppressed the expression of p-STAT3 and decreased SC-43-induced p-STAT3 inhibition (Fig. 9). These results indicated that relieved SHP-1 counteracts the SC-43-induced anti-CCA effect. SC-43, therefore, potentially relieves auto-inhibition of SHP-1, leading to p-STAT3 signal downregulation.

Effect of SC-43 on CCA xenograft tumor growth in vivo

In order to confirm that using SC-43 to inhibit p-STAT3 has potentially clinically relevant implications in CCA, we established a CCA xenograft model to evaluate the effect of SC-43 *in vivo*. In our study, SC-43 not only inhibited HuCCT-1 xenograft tumor size but also tumor weight significantly (Fig 10-A). The side effect of SC-43 was well-tolerated and no observable signs of toxicity were noted. All the experimental animals had stable body weights throughout the whole treatment course (Fig 10-B). The protein expression was checked to confirm the correlation between the biological response observed *in vivo* and the molecular mechanism discovered *in vitro*. The p-STAT3 level was reduced after SC-43 treatment. Moreover, SC-43 increased SHP-1 phosphatase activity compared with the control group (Fig 10-C). A schema summarizing the molecular mechanism of SC-43 in sensitive CCA cells is presented in Figure 11: SC-43 activates SHP-1 phosphatase by impairing the inhibitory N-SH2 domain, and contributes to p-STAT3, downstream cyclin B1 and Cdc2 downregulation, leading to G_2-M arrest and cancer cell apoptosis.

doi:10.6342/NTU202404281

3.2 Results in targeting PP5 study

PP5 enhances tumorigenesis of CCA

To evaluate the PP5 mRNA (*PPP5C*) expression in CCA, we analyzed the data obtained from TCGA, and found that levels of *PPP5C* were up-regulated in the tumor samples (Figure 12A, left). Although there was no significant difference among the stages of CCA, the *PPP5C* levels of CCA at different stages were higher than those of normal tissues (Figure 12A, right). We then ectopically expressed PP5 in HuCCT1 and KKU100, two CCA cell lines of human origin, to investigate whether PP5 may contribute to the tumorigenesis of CCA. As shown in Fig. 12B, overexpression of PP5 significantly accelerated proliferation of CCA cells. Results from the clonogenic assay (Fig. 13) and tumorsphere-formation assay (Fig. 14) also indicated that PP5 overexpression led to enhanced colony and tumorsphere formation.

PP5 knockdown suppresses tumor growth of CCA

Having established the correlation between PP5 overexpression and the growth advantage of CCA cells, we then sought to determine the impact of PP5 knockdown on CCA cell behavior. ShRNAs with two different sequences were employed to silence the expression of PP5 (Fig. 15) in HuCCT1 and KKU100 cells. Western blots showed that PP5-overexpressed CCA cells had p-AMPK downregulation, while PP5-knockdown cells with p-AMPK upregulation. Concomitant inhibition of cell growth was observed in CCA cells transfected with shRNAs against PP5 (Fig. 15). PP5 downregulation reduced PP5 activity (Fig. 16). PP5 knockdown also significantly impaired the clonogenic potential of KKU100 and HuCCT1 CCA cells (Fig. 17). To verify our findings from the *in vitro* studies, we established a subcutaneous HuCCT1 CCA mouse model. Viral particles that express shRNAs against PP5 were transduced to HuCCT1-bearing mice. Knockdown of PP5 expression led to reduced tumor volume (Fig. 18A) and decreased tumor weight (Fig. 18B). Compared to tumors from the control group, tumors from mice receiving PP5-targeting shRNAs

doi:10.6342/NTU202404281

exhibited approximately 50% reduction in both weight and size. Moreover, we collected the tumor lysates and carried out western blot analyses to identify the signaling molecules that contributed to protein phosphatase 5-regulated tumor growth. The expression of p-AMPK, a critical molecule that mediates cell growth and metabolism, was boosted in PP5-silenced tumor samples (Fig. 18C). These results imply that PP5 plays a critical role supporting CCA cell growth. PP5 knockdown reduced the volume and weight of CCA. AMPK may act as a downstream molecule of PP5 participating in CAA growth regulation.

CTD inhibits CCA cell survival with p-AMPK upregulation

We next explored whether PP5 could serve as a pharmacologically actionable target to treat CCA. HuCCT1, KKU100, and CGCCA cells treated with CTD, a known PP5 inhibitor, exhibited significantly diminished PP5 activity (Fig. 19A). Decreased cell viability (Fig. 19B) and increased apoptosis (Fig. 19C) were also found in CTD -treated CCA cells. Like CTD, NCTD treatment in CCA cells led to cell viability diminish in a time-dependent and concentration-dependent manner (Fig. 19B). Treating PP5-containing immunoprecipitant with CTD in cell-free settings also reduced PP5 activity, further confirming that CTD could be used to inhibit PP5 (Fig. 20). Furthermore, NCTD treatment induced a dose-dependent p-AMPK enhancement in CCA cells (Fig. 21). In addition, NCTD treatment in CCA cells decreased PP5 activity. (Fig. 22). To further confirm that PP5 modulates p-AMPK signals, CCA cells were first treated with CTD of different concentrations at different time points. As indicated in Fig. 23A, the expression of p-AMPK and its downstream molecule p-ACC, as well as cleaved Caspase-9 increased in a dose-dependent manner, upon CTD treatment. The upregulated signals of p-AMPK, p-ACC and cleaved PARP could be observed as soon as 8 hours post-CTD treatment (Fig. 23B). The data described above suggests that, by decreasing PP5 activity, CTD treatment resulted in increased CCA apoptosis with enhanced p-AMPK. PP5 may regulate p-AMPK signals, in a negative manner. Moreover, in vitro study, CTD treatment could

doi:10.6342/NTU202404281

upregulate p-ASK1 and p-JNK in CCA cells (Fig 24). Thus, CTD induced PP5 inhibition in CCA cells, leading to p-AMPK activation, and probably other downstream protein such as p-ASK1 and p-JNK.

PP5 promotes CCA cell survival through regulating AMPK signaling

We then investigated whether the CTD-induced cell death was mediated by PP5. Overexpression of PP5 rescued CCA cells from CTD-induced cell death (Fig. 25A), and the cleavage of caspase-9 and PARP, indicators of apoptosis, were also attenuated. On the other hand, the p-AMPK upregulation resulting from CTD treatment was compromised by PP5 overexpression. Arachidonic acid (AA), a PP5 activator, was also applied to CTD-treated CCA cells. The PP5 activator again reduced CTD treatment-induced p-AMPK expression, caspase-9 cleavage and apoptosis (Fig. 25B). To shed light on the role of AMPK in PP5-regulated CCA cell survival, AMPK was silenced by siRNA against AMPK. Knockdown of AMPK reduced the cleavage of Caspase-9 and PARP associated with PP5 activity inhibition by CTD treatment (Fig. 26A). Cell viability was also restored upon AMPK knockdown. Dorsomorphin dihydrochloride (compound C), an AMPK inhibitor, was also introduced to the CTD-treated CCA cells. Suppression of p-AMPK signals by the AMPK inhibitor mitigated cell apoptosis (Fig. 26B). HuCCT1 cells ectopically expressing PP5-DDK were immuneprecipitated using antibodies against DDK. Immunoblots performed thereafter using antibodies against AMPK confirmed that PP5 bound AMPK in CCA cells (Fig. 26C). Therefore, while CTD inhibits PP5 activity, it may not interfere with the association between PP5 and AMPK (Fig. 26C).

Pharmacologic inhibition of PP5 suppresses CCA tumor growth *in vivo*

To test whether the suppression of CCA growth by PP5 activity inhibition seen *in vitro* could be translated *in vivo*, HuCCT1-bearing mice were gavaged with NCTD (40 mg/kg), a less toxic

doi:10.6342/NTU202404281

analogue of CTD. PP5 IHC revealed decreased level in NCTD-treated tumor (Fig. 27). NCTD-treated tumor revealed decreased Ki67 expression. In contrast, NCTD treatment induced elevated TUNEL expression (Fig. 28). Similar result could be seen in vitro experiment that CTD downregulate proliferative marker such as Cyclin D1 and BrdU (Fig. 29). As revealed in Fig. 30A, mice administrated with NCTD showed significantly reduced tumor volume. No significant difference in body weight was observed between the control group and the NCTD treated mice (Fig. 30B). Compared with control group, NCTD-treated tumor revealed less dominant tumor part with increased stromal tissue (Fig 30C). Decreased PP5 activity (Fig. 31A) and increased p-AMPK expression (Fig. 31B) were detected in samples from the NCTD group. Figure 32 shows a working model of AMPK dephosphorylation by PP5 to promote CCA cancer development. PP5 induces CCA cell growth and tumor progression though dephosphorylation (inactivation) of AMPK, whereas PP5 inhibitor CTD suppresses tumor growth by increased p-AMPK. Taken together, data acquired by treatment with CTD and NCTD in this study support the concept that pharmacological inhibition of PP5 activity suppresses CCA growth.

doi:10.6342/NTU202404281

4. DISCUSSION

This thesis focuses on novel targeting agent discovery for CCA, which is one of the poorest prognosis cancer diseases with unmet medical need. It provides two proof-of-concept models from translational perspective. The first model showcases that targeting phosphorylated STAT3 by enhancing SHP-1 activity provide therapeutic effect for CCA, especially inflammatory-related CCA. The second model demonstrates that inhibiting PP5 activity with AMPK upregulation might be a potential treatment pathway. Followings are detailed discussion regarding our results on the hypothesis assessment.

4.1 Discussion in targeting SHP-1-STAT3 study

CCA is a fetal disease with dismal prognosis that lacks efficient medical management. There are few clinical trials incorporating molecularly targeted agents reported in this aggressive biliary tract malignancy. Therefore, novel treatment choice is of urgent need. In this article, we introduced a novel sorafenib derivative, SC-43, with potential therapeutic effects in CCA. We revealed that SC-43 demonstrates a significant anti-proliferative effect in CCA through p-STAT3 pathway inhibition. SHP-1 is a major determinant in the apoptosis effect of SC-43. By upregulating SHP-1, SC-43 induced SHP-1-dependent p-STAT3 downregulation. SC-43 directly interacts with SHP-1 SH2 domain and relieves its auto-inhibition structure. These findings not only increase current understanding of the SHP-1/STAT3 pathway but also support the rationale for targeting SHP-1 in the future development of therapies for CCA.

Chronic inflammation triggers cellular events that can promote malignant transformation of cells and carcinogenesis. Several inflammatory mediators, such as IL-6 and TGF-β, have been shown to participate in both the initiation and progression of cancer. STAT3 is crucial in initiating and maintaining a procarcinogenic inflammatory microenvironment, both at the beginning of malignant transformation and during further cancer progression.[57,58] IL-6/STAT3 remains a cornerstone factor

doi:10.6342/NTU202404281

regulating cholangiocyte growth and survival.[59,60] There is a growing body of evidence showing that IL-6/STAT3 signaling is clinically significant in CCA. Banchob et al. revealed that elevated IL-6 level after liver fluke *O.viverrini* infection correlated with formation of advanced periductal fibrosis, suggesting the importance of IL-6 signaling in CCA formation.[14] The expression of IL6 is upregulated in cancer cells and serum in patients with CCA.[61,62] Furthermore, expression of STAT3 is associated with poor histological differentiation and adverse prognosis in patients with CCA.[63] In this study, we demonstrated that p-STAT3 is a major target of SC-43, which is a sorafenib derivative without kinase inhibitor activity in CCA cells. The apoptosis of CCA cells after SC-43 administration is correlated with p-STAT3 downregulation, suggesting that STAT3 is a potential target in treating CCA.

Src homology region 2 (SH2) domain-containing phosphatase 1, SHP-1, acts as a negative regulator of phosphorylated STAT3 (p-STAT3). SHP-1 is a nonreceptor protein tyrosine phosphatase (PTP), composed of two SH2 domains that bind phosphotyrosine, a catalytic PTP domain, and a C-terminal tail. The phosphatase activity of SHP-1 depends on the variation of its 3D structure, as evidenced by its open- or closed-form chemical structure. The N-SH2 domain protrudes into the catalytic domain to directly block the entrance into the active site, and the highly mobile C-SH2 domain is thought to function as an antenna to search for the phosphopeptide activator.[64-66] Previously we demonstrated that SC-43 activates SHP-1 through direct interaction with SHP-1 proteins in breast cancer cells.[67] In the study on HCC cells, we provided a molecular docking model that sorafenib and SC-43 docked into the interface of N-SH2 and PTPase domain, we hypothesized that sorafenib and SC-43 could bind to the N-SH2 domain and subsequently releases and activates the PTPase domain. The interaction of sorafenib (or SC-43) and the N-SH2 domain might lead to a release of the D61 catalytic site and activation of SHP-1 activity. In current study, the hypothesized mechanism of SC-43 was supported by using dN1 (deleted N-SH2) and D61A mutant SHP-1- overexpressing cells; SC-43 exerted less p-STAT3 downregulation and apoptosis-inducing effects in these mutant SHP-1 over-expressing cells, compared to wild-type SHP-1-expressing cells. These results confirmed that the

doi:10.6342/NTU202404281

SH2 domain is a critical docking site of SC-43. However, given the fact that ectopic expression of STAT3 (thus increased p-STAT3) did not completely rescued the SC-43 induced apoptosis (Fig 2C), and that SHP-1 inhibitor PTP3 partially reduced the effect of SC-43 (Fig 4C), it is possible that there may also be other pathways involved in the effect of SC-43 induced apoptosis. Since SC-43 increases SHP-1 activity, it is reasonable that SC-43 induced effects can be mediated by other SHP-1-dependent substrates. Alternatively, other SHP-1 independent pathways may also be involved in SC-43 induced effects. More studies are needed to elucidate whether other pathways are also involved in SC-43 induced effects in CCA cells.

It is clear that the cell-cycle checkpoints can regulate the quality and rate of cell division. Agents that can increase G_2-M arrest have also been associated with enhanced apoptosis. For example, Jackson *et al.* [68] demonstrated that the Chk1 indolocarbazole inhibitor (SB-218078) enhanced G_2-M arrest and cytotoxicity in HeLa cells. Hirose *et al* [69] revealed that temozolamide induced G_2-M arrest-related apoptosis in glioma cells. With regards to the higher G_2-M arrest proportion, we hypothesized that SC-43 induced CCA cells apoptosis through G_2-M arrest. In our study, levels of expression of the cyclin B1 and Cdk1 (Cdc2), the major regulatory protein and kinase for progression from G_2 to M phase were markedly reduced after SC-43 treatment. It is known that stat3 signaling axis induced cell proliferation through binding to cdc2.[70-72] Furthermore, STAT3 promotes mitosis process primarily by stimulating transcription of cyclinB1 and other regulatory proteins, such as c-myc and cyclinD1.[73-77] In our presenting study, SC-43 induces apoptosis with downregulation of STAT3 in sensitive CCA cells. In addition, SC-43 promotes G_2-M arrest by reducing transcription level of cyclin B1 and Cdc2 protein.

SHP-1 is predominantly expressed in hematopoietic and epithelial cells. Notably, SHP-1 generally acts as a negative regulator in a variety of cellular signaling pathways.[78,79] However, the underlying molecular mechanism by which SHP-1 is involved in carcinogenesis is not completely understood. Some studies have indicated that SHP-1 is a potential tumor suppressor gene in cancer

doi:10.6342/NTU202404281

formation.[80-83] However, the clinical value of cancer treatment by targeting SHP-1 is still under investigation. According to a few reports,[84-86] several agents that regulate SHP-1 activity have been identified, and some have found efficacy against different cancer cells. In our previous work, we disclosed that regorafenib, a multiple protein kinase inhibitor, exerts anti-tumor effects by enhancing SHP-1 activity.[84] Dovitinib, another multiple protein kinase inhibitor, acts as a novel radiosensitizer in HCC by upregulating SHP-1.[85] Moreover, SHP-1 activation by a novel Bcl-2 inhibitor derivative was found to induce HCC autophagy.[86] In the present study, we demonstrated that SC-43 has a SHP-1-dependent apoptotic effect in CCA cells. Therefore, our data strengthen the rationale for targeting the SHP-1/STAT3 pathway as a novel anti-cancer therapy. Taken together, these structurally unrelated agents show a common target in various cancer cells suggesting that SHP-1 may be a potential therapeutic target.

In this study, a total of 40 cases with pathologically confirmed CCA were analyzed in this study. About half (21 of 40, 52.5%) of the specimens revealed only weak positive p-STAT3 expression. We have added Figure 33 showing some examples of weak-staining p-STAT3 in our CCA samples (Fig. 33). There are several possible reasons for the relatively low p-STAT3 expression in current study. First, the protein phosphorylation is usually dynamic and rapidly degraded. Second, the level of phosphorylated protein is relatively limited and difficultly detected. Third, the limitation of IHC for FFPE tissue due to the adverse influence of formalin upon antigenicity and the great variation in processing procedures. Fourth, in this retrospective study, some specimens have been preserved for more than ten years, therefore the quality of IHC in these FFPE tissue is inevitably diminished.

4.2 Discussion in targeting PP5 study

PP5 is a multifunctional signal regulator participating in cell-cycle control, DNA damage repair, stress response, and ion channel activation [39,87,88]. In this study, we explored the potential of PP5 as a therapeutic target in CCA. We confirmed that that overexpression of PP5 in CCA cells enhances cell

doi:10.6342/NTU202404281

growth, colony formation and sphere formation and, therefore, hypothesized that PP5 can act as an oncogenetic protein and might have an important role in CCA formation. Next, we employed shRNAs to genetically silence the expression of PP5, and NCTD to pharmacologically inhibit PP5 activity. The *in vivo* studies demonstrated that either silencing PP5 expression or inhibiting PP5 activity significantly reduced CCA tumor volume.

Several compounds exhibit PP5-inhibition activity, but most of them, including CTD and NCTD, also inhibit a broad spectrum of phosphatases belonging to the PPP family [89,90]. Highly-selective PP5 inhibitors are desired to avoid general toxicity. It has been indicated that the similarity of phosphatase catalytic elements among PPP family phosphatases may contribute in part to the non-specific inhibition [37,91]. On the other hand, improving PP5 inhibitors potency also attracted extensive interest. For example, limited interaction between PP5 inhibitors and Asp 99 residues in PP5 enhance inhibitors' activity [92]. Hence, the development of potent PP5 inhibitors with specificity might be beneficial for treating CCA.

A delicate balance of kinase phosphorylation and dephosphorylation, regulated by phosphoprotein phosphatase (PPP), is essential to the maintenance of diverse cellular function including proliferation, differentiation, senescence and apoptosis. AMPK is a serine/threonine protein kinase and has a critical role in many metabolic functions, including cellular energy homeostasis, protein synthesis, redox regulation and the anti-aging process [93-95]. Dysregulated AMPK is associated with many chronic diseases, such as obesity, inflammation and diabetes [96]. Under stress and energy deprivation, AMP and ADP bind to AMPK, causing phosphorylation at Thr 172 and leading to AMPK activation [94]. Moreover, AMPK activation is negatively controlled by phosphatases, namely PP2A and PP2C, by dephosphorylation at Thr 172 [97]. The data presented here suggests that PP5 also dephosphorylates AMPK at Thr 172. In addition, *in vitro* study revealed that CTD also upregulated p-ASK1 and p-JNK. It suggests that CTD inhibit PP5 and upregulate p-AMPK, and other downstream proteins such as p-ASK1 and p-JNK, leading to CCA cell apoptosis.

doi:10.6342/NTU202404281

Recently, the interaction between AMPK and cancer has been widely investigated. Urban G et al. reported that overexpression of PP5 in MCF-7 breast cancer cells enabled profound MCF-7 proliferation in estrogen-deprived culture media [40]. Interestingly, our data revealed that PP5 enhanced tumor cells colony and tumor sphere formation. Although this novel finding might be related to the cell proliferation promoting effect by PP5 and AMPK signaling, it also hinted to the possibility of correlation between PP5/AMPK and cancer stemness, which warrants future studies to elucidate the possibility. To date, the mechanism of AMPK activation in cancer cell inhibition is mainly depending on anti-inflammation [98] and mTOR pathway inhibition [99]. The use of metformin, an AMPK activator, in diabetic patients has been suggested to decrease cancer incidence [100]. Aspirin, another direct AMPK activator, is also used for cancer prevention [101]. Other AMPK activators have been shown to exhibit anti-cancer activity [102,103]. Moreover, Saengboonmee *et al.* reported that AMPK activation against CCA cells proliferation by STAT3 and NF-kB downregulation [104]. From a pharmacological point of view, we consider that the development of AMPK activators, perhaps by targeting the PP5-AMPK axis, for CCA therapy is a worthwhile future endeavor.

In conclusion, this study demonstrated that PP5 negatively regulates AMPK phosphorylation and contributes to CCA aggressiveness; it further indicates the potential of PP5 as a novel pharmacological actionable target for CCA therapy.

doi:10.6342/NTU202404281

5. CONCLUSION

In summary, we identified STAT3-SHP-1 as a major molecular determinant of the sensitivity of CCA cells to SC-43-induced apoptosis suggesting that it may be a potential drug target in CCA. The approach focusing on not only protein kinase, but also phosphatases and kinases could be a potential strategy for the management of CCA. Moreover, we showcase that PP5 induce tumorigenicity in CCA. Anti-tumor effect through PP5 downregulation was demonstrated by a potent PP5 inhibitor. This PP5-related therapeutic effect is regulated by AMPK phosphorylation.

doi:10.6342/NTU202404281

6. PERSPECTIVES

Based on our results, it is promising and feasible to develop novel agents for CCA treatment.

6.1 Defining SHP-1-p-STAT3 as a drug target and discovering agents targeting CIP2A-PP2A-p-Akt pathway.

SHP-1 consists of a catalytic domain at the C-terminus and two SH2 domains at the N-terminus, which bind to phosphotyrosines. An autoinhibitory conformation forms between the N-terminal SH2 domain and the catalytic PTP domain, with the catalytic PTP loop playing a crucial role in this autoinhibition, which is essential for SHP-1 phosphatase activity. Our data demonstrated that SC-43 may directly increase SHP-1 activity without altering SHP-1 expression phosphorylation, leading to p-STAT3 inhibition-related CCA treatment. Future studies exploring the clinical and biological roles of SHP-1 and p-STAT3 in CCA could enhance targeted therapies and further elucidate the therapeutic potential of p-STAT3 inhibitors. Additionally, it would be compelling to investigate whether other anti-inflammatory agents can contribute to the treatment of inflammatory cancers like CCA.

6.2 Dissect the underlying mechanisms by PP5 inhibition on the CCA treatment

The current results highlight the detailed role of PP5 in enhancing CCA tumorigenesis. PP5 negatively regulates AMPK phosphorylation and contributes to CCA aggressiveness. Accordingly, PP5 inhibition decreases CCA cell survival while upregulating p-AMPK, suggesting that PP5 is a potential pharmacologically actionable target for CCA therapy.

doi:10.6342/NTU202404281

7. REFERENCES

1. Welzel TM, McGlynn KA, Hsing AW, O'Brien TR, Pfeiffer RM. Impact of classification of hilar cholangiocarcinomas (Klatskin tumors) on the incidence of intra- and extrahepatic cholangiocarcinoma in the United States. *J Natl Cancer Inst.* 2006;98(12):873-875.
2. Brindley PJ, Bachini M, Ilyas SI, et al. Cholangiocarcinoma. *Nat Rev Dis Primers.* 2021;7(1):65.
3. Taylor-Robinson SD, Toledano MB, Arora S, et al. Increase in mortality rates from intrahepatic cholangiocarcinoma in England and Wales 1968-1998. *Gut.* 2001;48(6):816-820.
4. Banales JM, Marin JJG, Lamarca A, et al. Cholangiocarcinoma 2020: the next horizon in mechanisms and management. *Nat Rev Gastroenterol Hepatol.* 2020;17(9):557-588.
5. Valle JW, Kelley RK, Nervi B, Oh DY, Zhu AX. Biliary tract cancer. *Lancet.* 2021;397(10272):428-444.
6. Goyal L, Meric-Bernstam F, Hollebecque A, et al. Futibatinib for FGFR2-Rearranged Intrahepatic Cholangiocarcinoma. *N Engl J Med.* 2023;388(3):228-239.
7. Doebele RC, Drilon A, Paz-Ares L, et al. Entrectinib in patients with advanced or metastatic NTRK fusion-positive solid tumours: integrated analysis of three phase 1-2 trials. *Lancet Oncol.* 2020;21(2):271-282.
8. Marabelle A, Le DT, Ascierto PA, et al. Efficacy of Pembrolizumab in Patients With Noncolorectal High Microsatellite Instability/Mismatch Repair-Deficient Cancer: Results From the Phase II KEYNOTE-158 Study. *J Clin Oncol.* 2020;38(1):1-10.
9. Kelley RK, Ueno M, Yoo C, et al. Pembrolizumab in combination with gemcitabine and cisplatin compared with gemcitabine and cisplatin alone for patients with advanced biliary tract cancer (KEYNOTE-966): a randomised, double-blind, placebo-controlled, phase 3 trial. *Lancet.* 2023;401(10391):1853-1865.
10. Oh DY, He AR, Bouattour M, et al. Durvalumab or placebo plus gemcitabine and cisplatin in participants with advanced biliary tract cancer (TOPAZ-1): updated overall survival from a randomised phase 3 study. *Lancet Gastroenterol Hepatol.* 2024;9(8):694-704.
11. Everhart JE, Ruhl CE. Burden of digestive diseases in the United States Part III: Liver, biliary tract, and pancreas. *Gastroenterology.* 2009;136(4):1134-1144.
12. Izquierdo-Sanchez L, Lamarca A, La Casta A, et al. Cholangiocarcinoma landscape in Europe: Diagnostic, prognostic and therapeutic insights from the ENSCCA Registry. *J Hepatol.* 2022;76(5):1109-1121.
13. Honjo S, Srivatanakul P, Sriplung H, et al. Genetic and environmental determinants of risk for cholangiocarcinoma via Opisthorchis viverrini in a densely infested area in Nakhon Phanom, northeast Thailand. *Int J Cancer.* 2005;117(5):854-860.
14. Sripa B, Mairiang E, Thinkhamrop B, et al. Advanced periductal fibrosis from infection with the carcinogenic human liver fluke Opisthorchis viverrini correlates with elevated levels of interleukin-6. *Hepatology.* 2009;50(4):1273-1281.
15. Li H, Lan T, Liu H, et al. IL-6-induced cGGNBP2 encodes a protein to promote cell growth and metastasis in intrahepatic cholangiocarcinoma. *Hepatology.* 2022;75(6):1402-1419.
16. Schuringa JJ, Wierenga AT, Kruijer W, Vellenga E. Constitutive Stat3, Tyr705, and Ser727 phosphorylation in acute myeloid leukemia cells caused by the autocrine secretion of interleukin-6. *Blood.* 2000;95(12):3765-3770.
17. Meng F, Wehbe-Janek H, Henson R, Smith H, Patel T. Epigenetic regulation of microRNA-370 by interleukin-6 in malignant human cholangiocytes. *Oncogene.* 2008;27(3):378-386.
18. Landskron G, De la Fuente M, Thuwajit P, Thuwajit C, Hermoso MA. Chronic inflammation and cytokines in the tumor microenvironment. *Journal of immunology research.* 2014;2014:149185.
19. Rodrigues PM, Olaizola P, Paiva NA, et al. Pathogenesis of Cholangiocarcinoma. *Annu Rev*

doi:10.6342/NTU202404281

Pathol. 2021;16:433-463.
20. Sun L, Wang Y, Cen J, et al. Modelling liver cancer initiation with organoids derived from directly reprogrammed human hepatocytes. *Nat Cell Biol.* 2019;21(8):1015-1026.
21. Wang S, Yadav AK, Han JY, Ahn KS, Jang BC. Anti-Growth, Anti-Angiogenic, and Pro-Apoptotic Effects by CX-4945, an Inhibitor of Casein Kinase 2, on HuCCT-1 Human Cholangiocarcinoma Cells via Control of Caspase-9/3, DR-4, STAT-3/STAT-5, Mcl-1, eIF-2alpha, and HIF-1alpha. *Int J Mol Sci.* 2022;23(11).
22. Zou S, Tong Q, Liu B, Huang W, Tian Y, Fu X. Targeting STAT3 in Cancer Immunotherapy. *Mol Cancer.* 2020;19(1):145.
23. Verstovsek S, Mesa RA, Gotlib J, et al. A double-blind, placebo-controlled trial of ruxolitinib for myelofibrosis. *N Engl J Med.* 2012;366(9):799-807.
24. Moon SY, Lee H, Kim S, et al. Inhibition of STAT3 enhances sensitivity to tamoxifen in tamoxifen-resistant breast cancer cells. *BMC Cancer*. 2021;21(1):931.
25. Xu J, Lin H, Wu G, Zhu M, Li M. IL-6/STAT3 Is a Promising Therapeutic Target for Hepatocellular Carcinoma. *Front Oncol.* 2021;11:760971.
26. Di JX, Zhang HY. C188-9, a small-molecule STAT3 inhibitor, exerts an antitumor effect on head and neck squamous cell carcinoma. *Anticancer Drugs.* 2019;30(8):846-853.
27. Jung KH, Yoo W, Stevenson HL, et al. Multifunctional Effects of a Small-Molecule STAT3 Inhibitor on NASH and Hepatocellular Carcinoma in Mice. *Clin Cancer Res.* 2017;23(18):5537-5546.
28. Blechacz BR, Smoot RL, Bronk SF, Werneburg NW, Sirica AE, Gores GJ. Sorafenib inhibits signal transducer and activator of transcription-3 signaling in cholangiocarcinoma cells by activating the phosphatase shatterproof 2. *Hepatology.* 2009;50(6):1861-1870.
29. Tai WT, Shiau CW, Chen PJ, et al. Discovery of novel Src homology region 2 domain-containing phosphatase 1 agonists from sorafenib for the treatment of hepatocellular carcinoma. *Hepatology.* 2014;59(1):190-201.
30. Tai WT, Cheng AL, Shiau CW, et al. Signal transducer and activator of transcription 3 is a major kinase-independent target of sorafenib in hepatocellular carcinoma. *Journal of hepatology.* 2011;55(5):1041-1048.
31. Graves JD, Krebs EG. Protein phosphorylation and signal transduction. *Pharmacol Ther.* 1999;82(2-3):111-121.
32. Manning G, Whyte DB, Martinez R, Hunter T, Sudarsanam S. The protein kinase complement of the human genome. *Science.* 2002;298(5600):1912-1934.
33. Turdo A, D'Accardo C, Glaviano A, et al. Targeting Phosphatases and Kinases: How to Checkmate Cancer. *Front Cell Dev Biol.* 2021;9:690306.
34. Liu J, Ren G, Li K, et al. The Smad4-MYO18A-PP1A complex regulates beta-catenin phosphorylation and pemigatinib resistance by inhibiting PAK1 in cholangiocarcinoma. *Cell Death Differ.* 2022;29(4):818-831.
35. Jiang TY, Shi YY, Cui XW, et al. PTEN Deficiency Facilitates Exosome Secretion and Metastasis in Cholangiocarcinoma by Impairing TFEB-mediated Lysosome Biogenesis. *Gastroenterology.* 2023;164(3):424-438.
36. Chida K, Kawazoe A, Kawazu M, et al. A Low Tumor Mutational Burden and PTEN Mutations Are Predictors of a Negative Response to PD-1 Blockade in MSI-H/dMMR Gastrointestinal Tumors. *Clin Cancer Res.* 2021;27(13):3714-3724.
37. Swingle MR, Honkanen RE, Ciszak EM. Structural basis for the catalytic activity of human serine/threonine protein phosphatase-5. *J Biol Chem.* 2004;279(32):33992-33999.
38. Yang J, Roe SM, Cliff MJ, et al. Molecular basis for TPR domain-mediated regulation of protein phosphatase 5. *EMBO J.* 2005;24(1):1-10.
39. Golden T, Swingle M, Honkanen RE. The role of serine/threonine protein phosphatase type 5 (PP5) in the regulation of stress-induced signaling networks and cancer. *Cancer*

doi:10.6342/NTU202404281

Metastasis Rev. 2008;27(2):169-178.
40. Urban G, Golden T, Aragon IV, Scammell JG, Dean NM, Honkanen RE. Identification of an estrogen-inducible phosphatase (PP5) that converts MCF-7 human breast carcinoma cells into an estrogen-independent phenotype when expressed constitutively. *J Biol Chem.* 2001;276(29):27638-27646.
41. Shao J, Hartson SD, Matts RL. Evidence that protein phosphatase 5 functions to negatively modulate the maturation of the Hsp90-dependent heme-regulated eIF2alpha kinase. *Biochemistry.* 2002;41(21):6770-6779.
42. Shah BH, Catt KJ. Protein phosphatase 5 as a negative key regulator of Raf-1 activation. *Trends Endocrinol Metab.* 2006;17(10):382-384.
43. Zhou G, Golden T, Aragon IV, Honkanen RE. Ser/Thr protein phosphatase 5 inactivates hypoxia-induced activation of an apoptosis signal-regulating kinase 1/MKK-4/JNK signaling cascade. *J Biol Chem.* 2004;279(45):46595-46605.
44. Zuo Z, Urban G, Scammell JG, et al. Ser/Thr protein phosphatase type 5 (PP5) is a negative regulator of glucocorticoid receptor-mediated growth arrest. *Biochemistry.* 1999;38(28):8849-8857.
45. Zhi X, Zhang H, He C, Wei Y, Bian L, Li G. Serine/Threonine Protein Phosphatase-5 Accelerates Cell Growth and Migration in Human Glioma. *Cell Mol Neurobiol.* 2015;35(5):669-677.
46. Feng L, Sun P, Li Z, Liu M, Sun S. Knockdown of PPP5C inhibits growth of hepatocellular carcinoma cells in vitro. *Appl Biochem Biotechnol.* 2015;175(1):526-534.
47. Zheng X, Zhang L, Jin B, Zhang F, Zhang D, Cui L. Knockdown of protein phosphatase 5 inhibits ovarian cancer growth in vitro. *Oncol Lett.* 2016;11(1):168-172.
48. Carrel JE, Doom JP, McCormick JP. Identification of cantharidin in false blister beetles (Coleoptera, Oedemeridae) from florida. *J Chem Ecol.* 1986;12(3):741-747.
49. Li YM, Casida JE. Cantharidin-binding protein: identification as protein phosphatase 2A. *Proc Natl Acad Sci U S A.* 1992;89(24):11867-11870.
50. Wang GS. Medical uses of mylabris in ancient China and recent studies. *J Ethnopharmacol.* 1989;26(2):147-162.
51. Dorn DC, Kou CA, Png KJ, Moore MA. The effect of cantharidins on leukemic stem cells. *Int J Cancer.* 2009;124(9):2186-2199.
52. Karras DJ, Farrell SE, Harrigan RA, Henretig FM, Gealt L. Poisoning from "Spanish fly" (cantharidin). *Am J Emerg Med.* 1996;14(5):478-483.
53. Miyagiwa M, Ichida T, Tokiwa T, Sato J, Sasaki H. A new human cholangiocellular carcinoma cell line (HuCC-T1) producing carbohydrate antigen 19/9 in serum-free medium. *In Vitro Cell Dev Biol.* 1989;25(6):503-510.
54. Sripa B, Leungwattanawanit S, Nitta T, et al. Establishment and characterization of an opisthorchiasis-associated cholangiocarcinoma cell line (KKU-100). *World J Gastroenterol.* 2005;11(22):3392-3397.
55. Chen MH, Chiang KC, Cheng CT, et al. Antitumor activity of the combination of an HSP90 inhibitor and a PI3K/mTOR dual inhibitor against cholangiocarcinoma. *Oncotarget.* 2014;5(9):2372-2389.
56. Yeh CN, Chiang KC, Juang HH, et al. Reappraisal of the therapeutic role of celecoxib in cholangiocarcinoma. *PLoS One.* 2013;8(7):e69928.
57. Mantovani A, Allavena P, Sica A, Balkwill F. Cancer-related inflammation. *Nature.* 2008;454(7203):436-444.
58. Catlett-Falcone R, Landowski TH, Oshiro MM, et al. Constitutive activation of Stat3 signaling confers resistance to apoptosis in human U266 myeloma cells. *Immunity.* 1999;10(1):105-115.
59. Matsumoto K, Fujii H, Michalopoulos G, Fung JJ, Demetris AJ. Human biliary epithelial

doi:10.6342/NTU202404281

cells secrete and respond to cytokines and hepatocyte growth factors in vitro: interleukin-6, hepatocyte growth factor and epidermal growth factor promote DNA synthesis in vitro. *Hepatology.* 1994;20(2):376-382.
60. Meng F, Yamagiwa Y, Ueno Y, Patel T. Over-expression of interleukin-6 enhances cell survival and transformed cell growth in human malignant cholangiocytes. *Journal of hepatology.* 2006;44(6):1055-1065.
61. Yokomuro S, Tsuji H, Lunz JG, 3rd, et al. Growth control of human biliary epithelial cells by interleukin 6, hepatocyte growth factor, transforming growth factor beta1, and activin A: comparison of a cholangiocarcinoma cell line with primary cultures of non-neoplastic biliary epithelial cells. *Hepatology.* 2000;32(1):26-35.
62. Nehls O, Gregor M, Klump B. Serum and bile markers for cholangiocarcinoma. *Seminars in liver disease.* 2004;24(2):139-154.
63. Dokduang H, Techasen A, Namwat N, et al. STATs profiling reveals predominantly-activated STAT3 in cholangiocarcinoma genesis and progression. *Journal of hepato-biliary-pancreatic sciences.* 2014;21(10):767-776.
64. Yang J, Liang X, Niu T, Meng W, Zhao Z, Zhou GW. Crystal structure of the catalytic domain of protein-tyrosine phosphatase SHP-1. *The Journal of biological chemistry.* 1998;273(43):28199-28207.
65. Yang J, Liu L, He D, et al. Crystal structure of human protein-tyrosine phosphatase SHP-1. *The Journal of biological chemistry.* 2003;278(8):6516-6520.
66. Wang W, Liu L, Song X, et al. Crystal structure of human protein tyrosine phosphatase SHP-1 in the open conformation. *Journal of cellular biochemistry.* 2011;112(8):2062-2071.
67. Liu CY, Tseng LM, Su JC, et al. Novel sorafenib analogues induce apoptosis through SHP-1 dependent STAT3 inactivation in human breast cancer cells. *Breast Cancer Res.* 2013;15(4):R63.
68. Jackson JR, Gilmartin A, Imburgia C, Winkler JD, Marshall LA, Roshak A. An indolocarbazole inhibitor of human checkpoint kinase (Chk1) abrogates cell cycle arrest caused by DNA damage. *Cancer research.* 2000;60(3):566-572.
69. Hirose Y, Berger MS, Pieper RO. Abrogation of the Chk1-mediated G(2) checkpoint pathway potentiates temozolomide-induced toxicity in a p53-independent manner in human glioblastoma cells. *Cancer research.* 2001;61(15):5843-5849.
70. O'Connor DS, Grossman D, Plescia J, et al. Regulation of apoptosis at cell division by p34cdc2 phosphorylation of survivin. *Proceedings of the National Academy of Sciences of the United States of America.* 2000;97(24):13103-13107.
71. Altieri DC. Survivin, cancer networks and pathway-directed drug discovery. *Nature reviews Cancer.* 2008;8(1):61-70.
72. Bollrath J, Phesse TJ, von Burstin VA, et al. gp130-mediated Stat3 activation in enterocytes regulates cell survival and cell-cycle progression during colitis-associated tumorigenesis. *Cancer cell.* 2009;15(2):91-102.
73. Jarnicki A, Putoczki T, Ernst M. Stat3: linking inflammation to epithelial cancer - more than a "gut" feeling? *Cell division.* 2010;5:14.
74. Liu T, Peng H, Zhang M, Deng Y, Wu Z. Cucurbitacin B, a small molecule inhibitor of the Stat3 signaling pathway, enhances the chemosensitivity of laryngeal squamous cell carcinoma cells to cisplatin. *European journal of pharmacology.* 2010;641(1):15-22.
75. Bromberg JF, Wrzeszczynska MH, Devgan G, et al. Stat3 as an oncogene. *Cell.* 1999;98(3):295-303.
76. Masuda M, Suzui M, Yasumatu R, et al. Constitutive activation of signal transducers and activators of transcription 3 correlates with cyclin D1 overexpression and may provide a novel prognostic marker in head and neck squamous cell carcinoma. *Cancer research.* 2002;62(12):3351-3355.

doi:10.6342/NTU202404281

77. Bowman T, Broome MA, Sinibaldi D, et al. Stat3-mediated Myc expression is required for Src transformation and PDGF-induced mitogenesis. *Proceedings of the National Academy of Sciences of the United States of America.* 2001;98(13):7319-7324.
78. Neel BG, Tonks NK. Protein tyrosine phosphatases in signal transduction. *Current opinion in cell biology.* 1997;9(2):193-204.
79. Barford D, Neel BG. Revealing mechanisms for SH2 domain mediated regulation of the protein tyrosine phosphatase SHP-2. *Structure.* 1998;6(3):249-254.
80. Hegazy SA, Wang P, Anand M, Ingham RJ, Gelebart P, Lai R. The tyrosine 343 residue of nucleophosmin (NPM)-anaplastic lymphoma kinase (ALK) is important for its interaction with SHP1, a cytoplasmic tyrosine phosphatase with tumor suppressor functions. *The Journal of biological chemistry.* 2010;285(26):19813-19820.
81. Witkiewicz A, Raghunath P, Wasik A, et al. Loss of SHP-1 tyrosine phosphatase expression correlates with the advanced stages of cutaneous T-cell lymphoma. *Human pathology.* 2007;38(3):462-467.
82. Hayslip J, Montero A. Tumor suppressor gene methylation in follicular lymphoma: a comprehensive review. *Molecular cancer.* 2006;5:44.
83. Chim CS, Wong KY, Loong F, Srivastava G. SOCS1 and SHP1 hypermethylation in mantle cell lymphoma and follicular lymphoma: implications for epigenetic activation of the Jak/STAT pathway. *Leukemia.* 2004;18(2):356-358.
84. Fan LC, Teng HW, Shiau CW, et al. SHP-1 is a target of regorafenib in colorectal cancer. *Oncotarget.* 2014;5(15):6243-6251.
85. Huang CY, Tai WT, Wu SY, et al. Dovitinib Acts As a Novel Radiosensitizer in Hepatocellular Carcinoma by Targeting SHP-1/STAT3 Signaling. *International journal of radiation oncology, biology, physics.* 2016.
86. Su JC, Tseng PH, Hsu CY, et al. RFX1-dependent activation of SHP-1 induces autophagy by a novel obatoclax derivative in hepatocellular carcinoma cells. *Oncotarget.* 2014;5(13):4909-4919.
87. Oberoi J, Dunn DM, Woodford MR, et al. Structural and functional basis of protein phosphatase 5 substrate specificity. *Proc Natl Acad Sci U S A.* 2016;113(32):9009-9014.
88. von Kriegsheim A, Pitt A, Grindlay GJ, Kolch W, Dhillon AS. Regulation of the Raf-MEK-ERK pathway by protein phosphatase 5. *Nat Cell Biol.* 2006;8(9):1011-1016.
89. Swingle M, Ni L, Honkanen RE. Small-molecule inhibitors of ser/thr protein phosphatases: specificity, use and common forms of abuse. *Methods Mol Biol.* 2007;365:23-38.
90. Puerto Galvis CE, Vargas Mendez LY, Kouznetsov VV. Cantharidin-based small molecules as potential therapeutic agents. *Chem Biol Drug Des.* 2013;82(5):477-499.
91. Hong TJ, Park K, Choi EW, Hahn JS. Ro 90-7501 inhibits PP5 through a novel, TPR-dependent mechanism. *Biochem Biophys Res Commun.* 2017;482(2):215-220.
92. Liu JY, Chen XE, Zhang YL. Insights into the key interactions between human protein phosphatase 5 and cantharidin using molecular dynamics and site-directed mutagenesis bioassays. *Sci Rep.* 2015;5:12359.
93. Oakhill JS, Scott JW, Kemp BE. AMPK functions as an adenylate charge-regulated protein kinase. *Trends Endocrinol Metab.* 2012;23(3):125-132.
94. Hardie DG, Ross FA, Hawley SA. AMPK: a nutrient and energy sensor that maintains energy homeostasis. *Nat Rev Mol Cell Biol.* 2012;13(4):251-262.
95. Hardie DG, Ross FA, Hawley SA. AMP-activated protein kinase: a target for drugs both ancient and modern. *Chem Biol.* 2012;19(10):1222-1236.
96. Jeon SM. Regulation and function of AMPK in physiology and diseases. *Exp Mol Med.* 2016;48(7):e245.
97. Kjobsted R, Wojtaszewski JF, Treebak JT. Role of AMP-Activated Protein Kinase for Regulating Post-exercise Insulin Sensitivity. *EXS.* 2016;107:81-126.

doi:10.6342/NTU202404281

98. O'Neill LA, Hardie DG. Metabolism of inflammation limited by AMPK and pseudo-starvation. *Nature.* 2013;493(7432):346-355.
99. Xu J, Ji J, Yan XH. Cross-talk between AMPK and mTOR in regulating energy balance. *Crit Rev Food Sci Nutr.* 2012;52(5):373-381.
100. Evans JM, Donnelly LA, Emslie-Smith AM, Alessi DR, Morris AD. Metformin and reduced risk of cancer in diabetic patients. *BMJ.* 2005;330(7503):1304-1305.
101. Cuzick J, Otto F, Baron JA, et al. Aspirin and non-steroidal anti-inflammatory drugs for cancer prevention: an international consensus statement. *Lancet Oncol.* 2009;10(5):501-507.
102. Lee KH, Hsu EC, Guh JH, et al. Targeting energy metabolic and oncogenic signaling pathways in triple-negative breast cancer by a novel adenosine monophosphate-activated protein kinase (AMPK) activator. *J Biol Chem.* 2011;286(45):39247-39258.
103. Zadra G, Photopoulos C, Tyekucheva S, et al. A novel direct activator of AMPK inhibits prostate cancer growth by blocking lipogenesis. *EMBO Mol Med.* 2014;6(4):519-538.
104. Saengboonmee C, Seubwai W, Cha'on U, Sawanyawisuth K, Wongkham S, Wongkham C. Metformin Exerts Antiproliferative and Anti-metastatic Effects Against Cholangiocarcinoma Cells by Targeting STAT3 and NF-kB. *Anticancer Res.* 2017;37(1):115-123.

doi:10.6342/NTU202404281

Figures

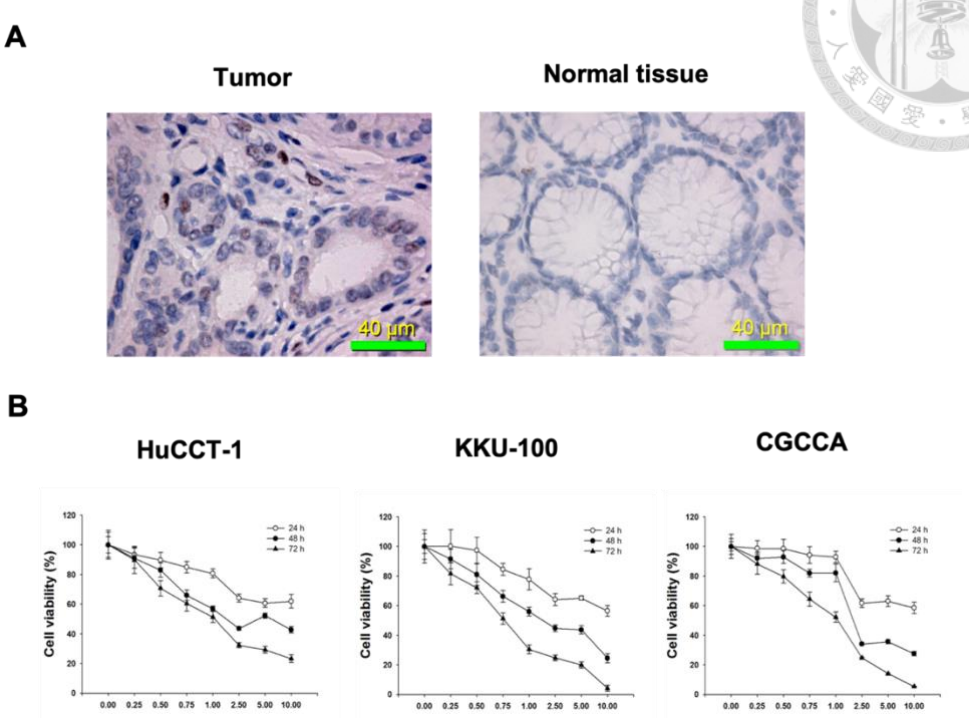

Figure 1. SC-43 exerts anti-proliferative and apoptosis-inducing effects in cholangiocarcinoma (CCA) cells. SC-43, a derivative of sorafenib induces apoptosis in CCA cell lines. A, immunohistochemical (IHC) staining for p-STAT3 in CCA tumor (left), compared with normal tissue part (right). B, dose-escalation effects of SC-43 on cell viability. Cells were exposed to SC-43 at the indicated doses for 24, 48, and 72 hours respectively and cell viability was assessed by MTT assay. Points, mean; bars, SD (*n*=9).

doi:10.6342/NTU202404281

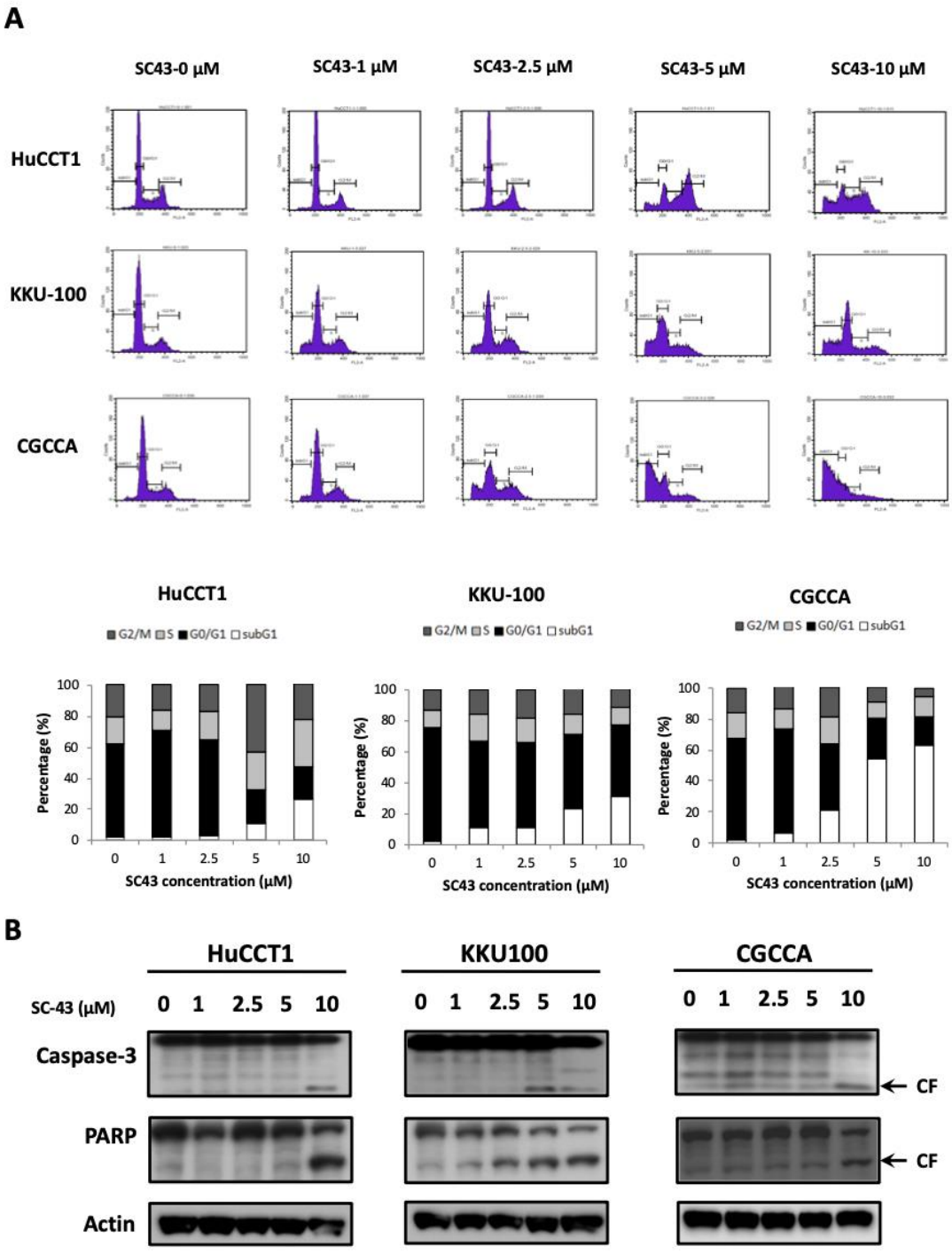

Figure 2. SC-43 exerts apoptotic effects in CCA cells. A. CCA cells were exposed to SC-43 at the indicated doses for 24 hours and number of apoptotic cells was determined by flow cytometry. Columns, mean; bars, SD (*n*=3). B. Dose-dependent effects of SC-42 on cleaved caspase-3 and PARP Cell were treated with SC-43 at the indicated doses for 24 hours.

doi:10.6342/NTU202404281

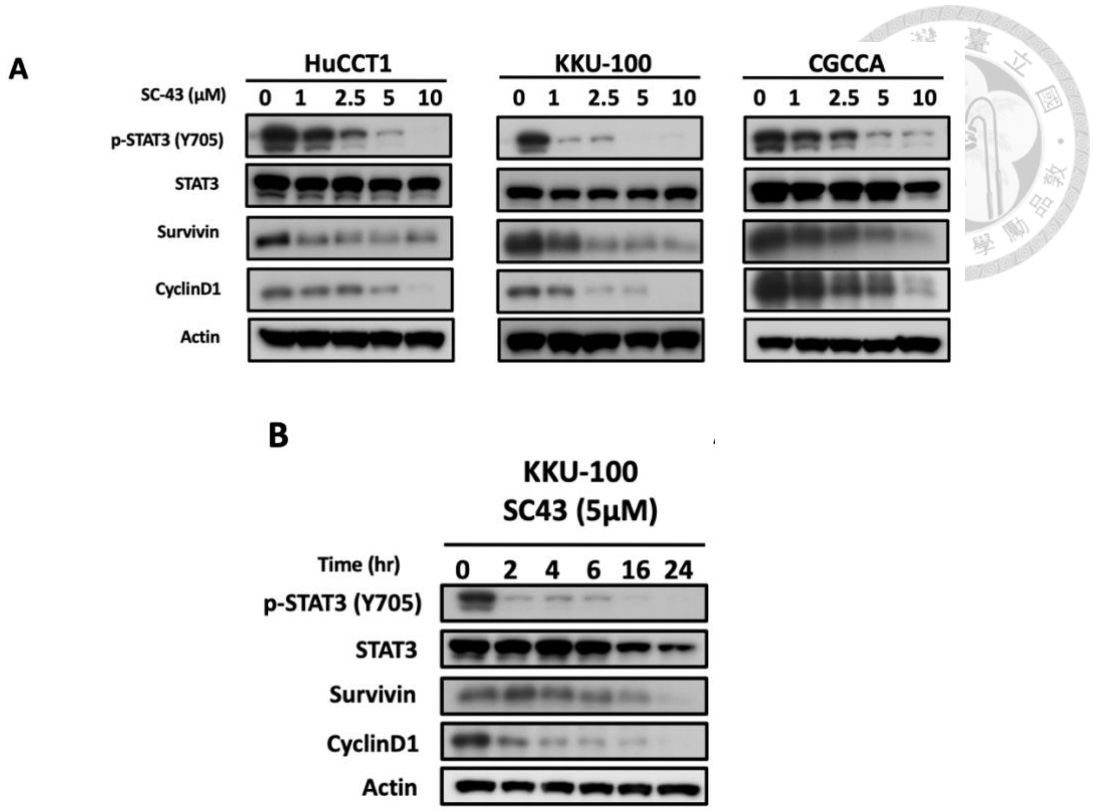

Figure 3. Inhibition of p-STAT3 determines the sensitizing effects of SC-43 in CCA cells. A, dose-dependent effects of SC-43 on STAT3-related proteins. Cell were treated with SC-43 at the indicated doses for 24 hours. B, SC-43 induced p-STAT3 inactivation in a time-dependent manner.

doi:10.6342/NTU202404281

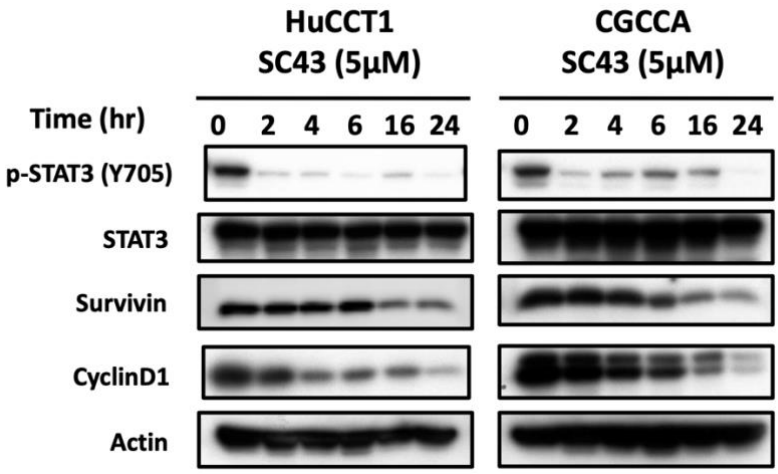

Figure 4. Consistent inhibition of p-STAT3 of SC-43 in CCA cells. SC-43 induced p-STAT3 inactivation of HuCCT1 and CGCCA cells in a time-dependent manner.

doi:10.6342/NTU202404281

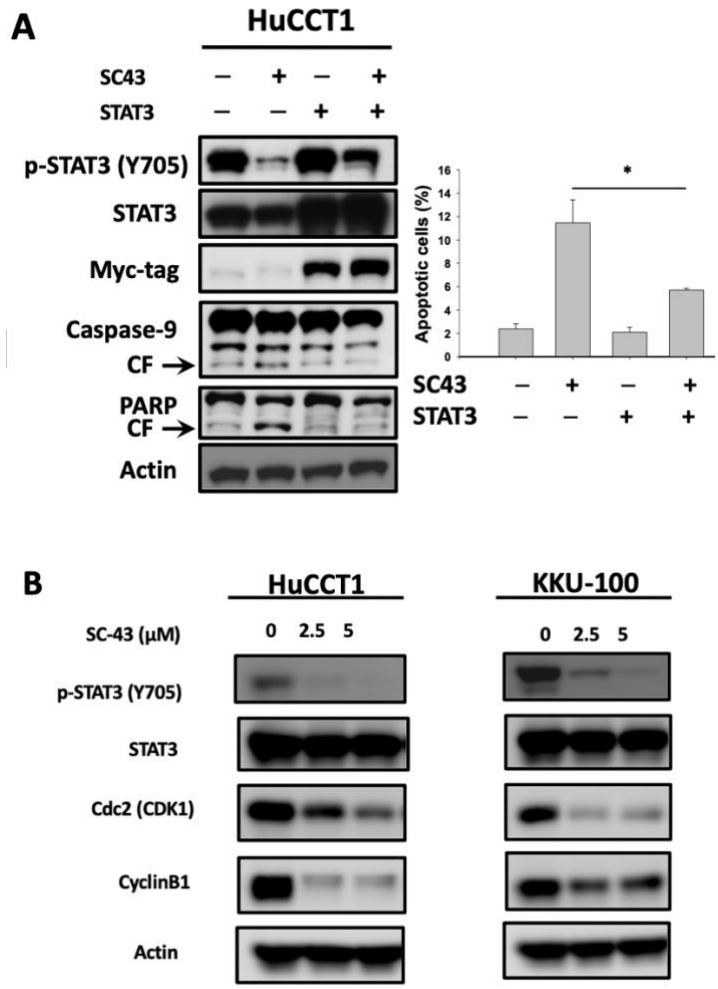

Figure 5. SC-43 induce STAT-3-related G_2-M arrest in CCA cells. A. STAT3 reverses the apoptotic effect of SC-43. HuCCT-1 cells transiently expressing STAT3 with Myc-tag were treated with SC-43 at 5 μM for 24 hours and the percentage of apoptosis was measured by sub-G1 analysis. B. Western blot analysis of the cyclin B1 and Cdk1 (Cdc2) with SC-43 at the indicated doses for 24 hours. Columns, mean; bars, SD (n=3); *, $P < 0.05$.

doi:10.6342/NTU202404281

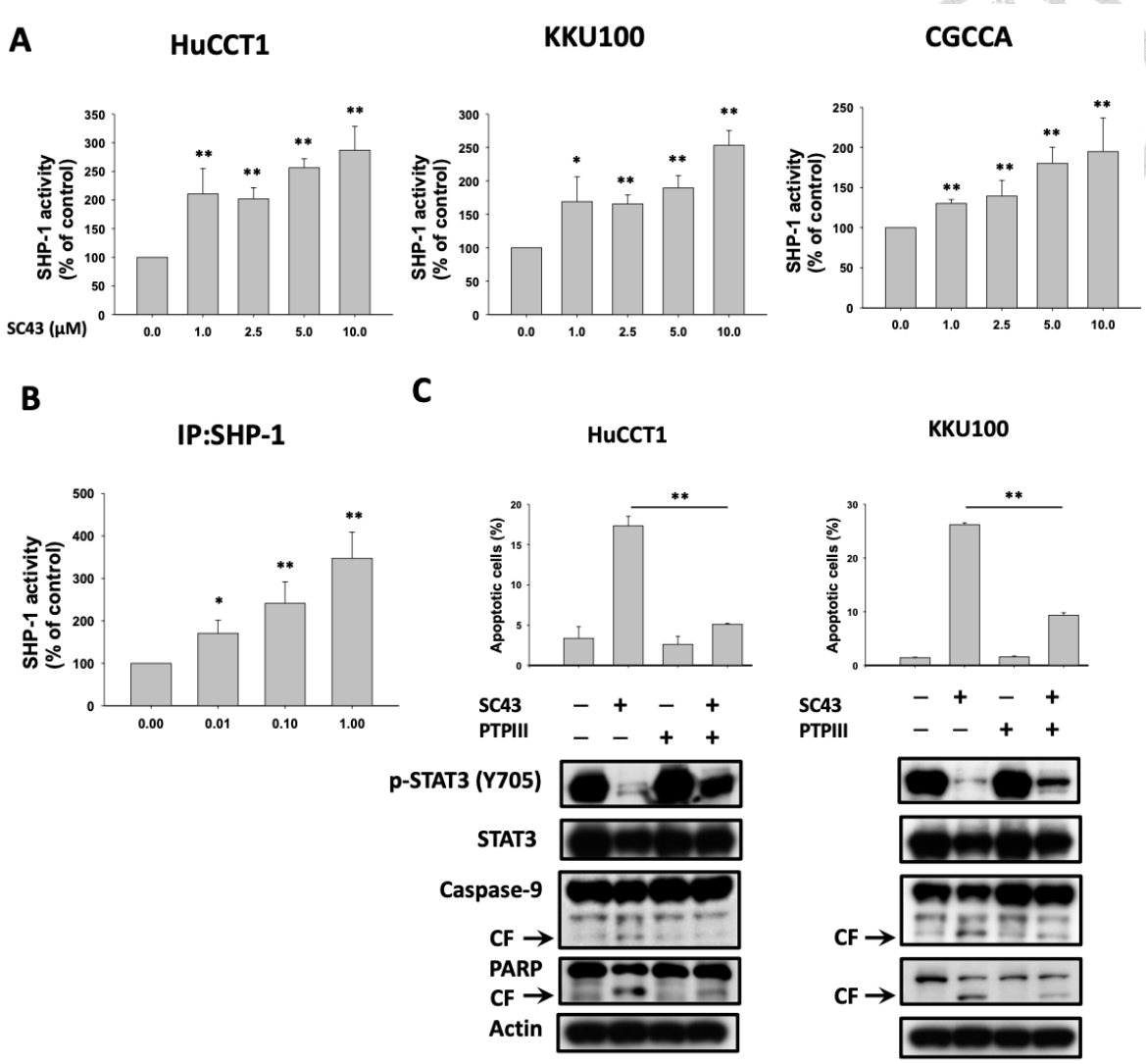

Figure 6. SHP-1/p-STAT3 mediates SC-43-induced apoptosis in CCA cells. SHP-1 plays a role in SC-43-induced STAT3 inhibition and apoptosis. A, SC-43 increased SHP-1 activity in CCA cells. Cells were treated with SC-43 at the indicated doses for 16 hours. Columns, mean; bars, SD (n=3). (*, $P < 0.05$; **, $P < 0.01$) B, SC-43 activates SHP-1 directly. SC-43 increases the phosphatase activity of SHP-1 in IP-SHP-1 cell lysate from HuCCT-1 cells. Columns, mean; bars, SD (n=3). (*, $P < 0.05$; **, $P < 0.01$) C, Protective effects of SHP-1 specific inhibitor (PTPIII) on SC-43-induced apoptosis in HuCCT-1 and KKU-100 cells. Cells were pretreated with PTPIII at 100 nM for 30 minutes before SC-43 treatment.

doi:10.6342/NTU202404281

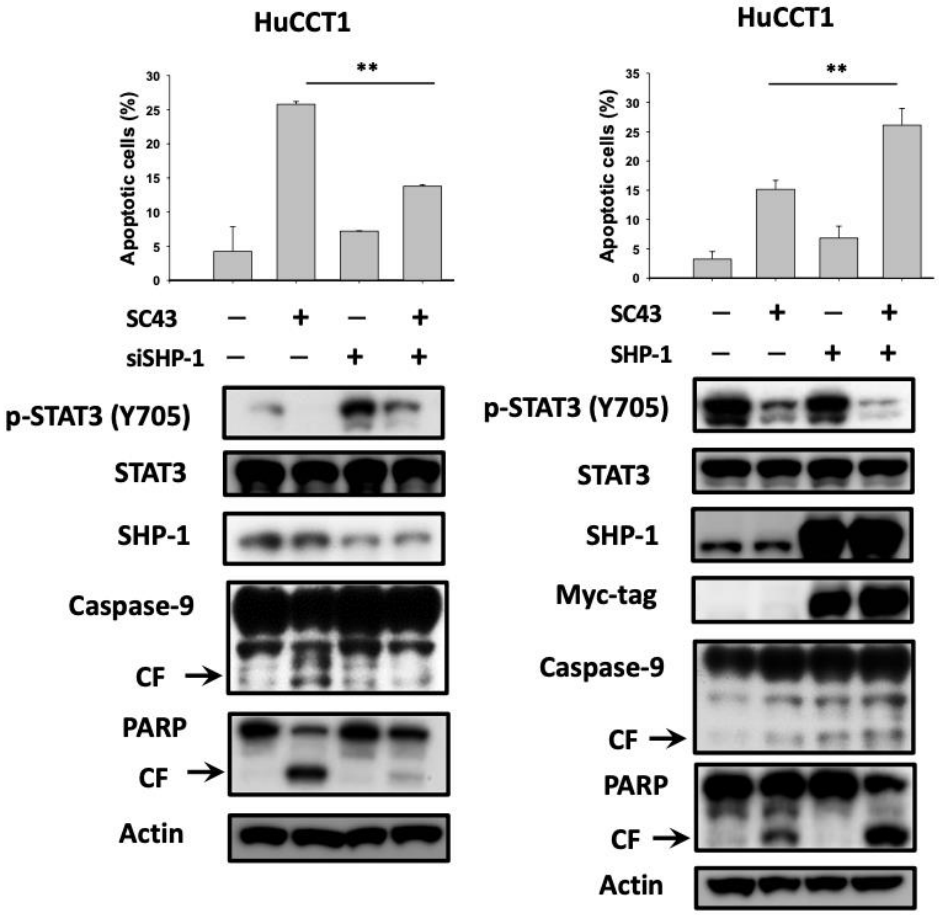

Figure 7. SHP-1 activity on p-STAT3-related apoptosis in CCA cells. Knockdown of SHP-1 reduces the effects of SC-43 on p-STAT3 and apoptosis. HuCCT-1 cells were transfected with control siRNA or SHP-1 siRNA for 24 hours and then treated with SC-43 for another 24 hours (left). Overexpression of SHP-1 induces more apoptosis with SC-43. Apoptotic assay was performed by sub-G1 analysis (right). Columns, mean; bars, SD (n=3). (**, $P < 0.01$)

doi:10.6342/NTU202404281

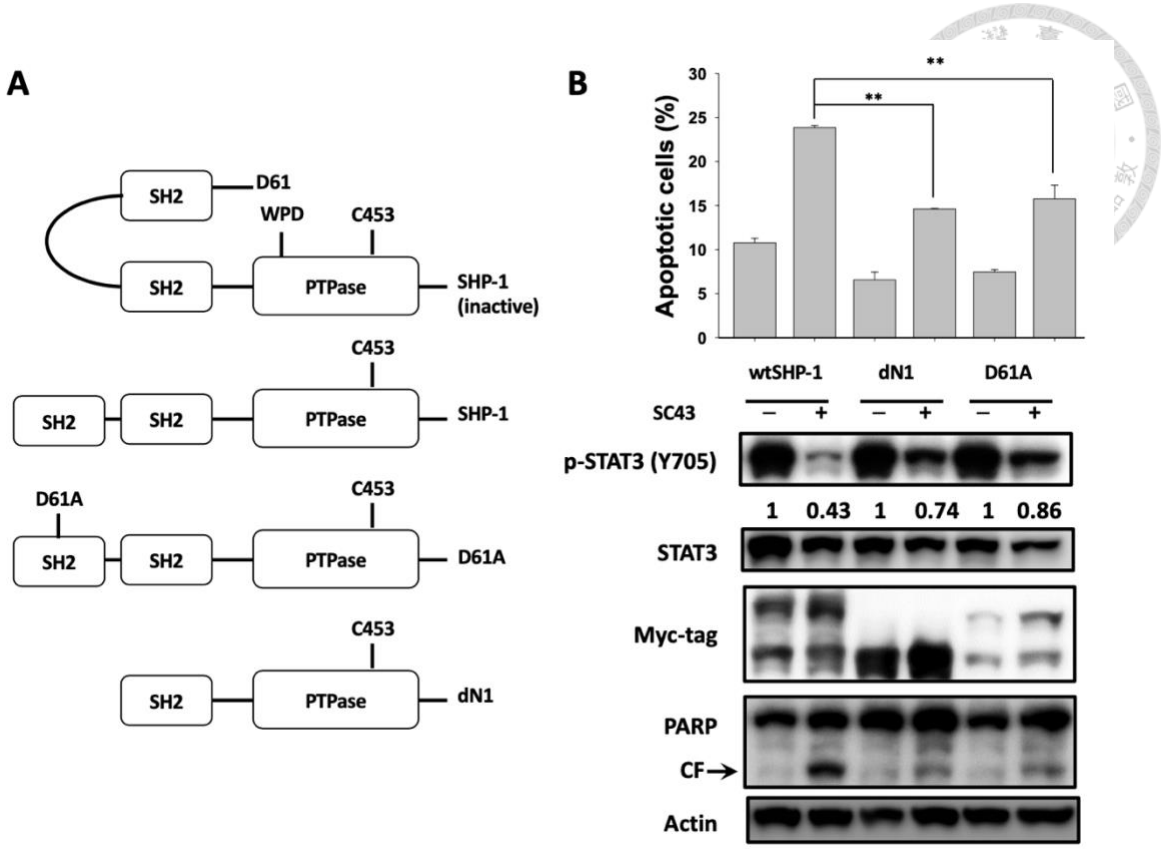

Figure 8. SC-43 activates SHP-1 by relieving the autoinhibition of the SH2 domain. A. Schematic representation of deletion and single mutants of SHP-1. B. dN1 and D61A impair SC-43-induced STAT3 signaling and apoptotic effect. Apoptotic assay was performed by sub-G1 analysis. Columns, mean; bars, SD (n=3). (**, $P < 0.01$)

doi:10.6342/NTU202404281

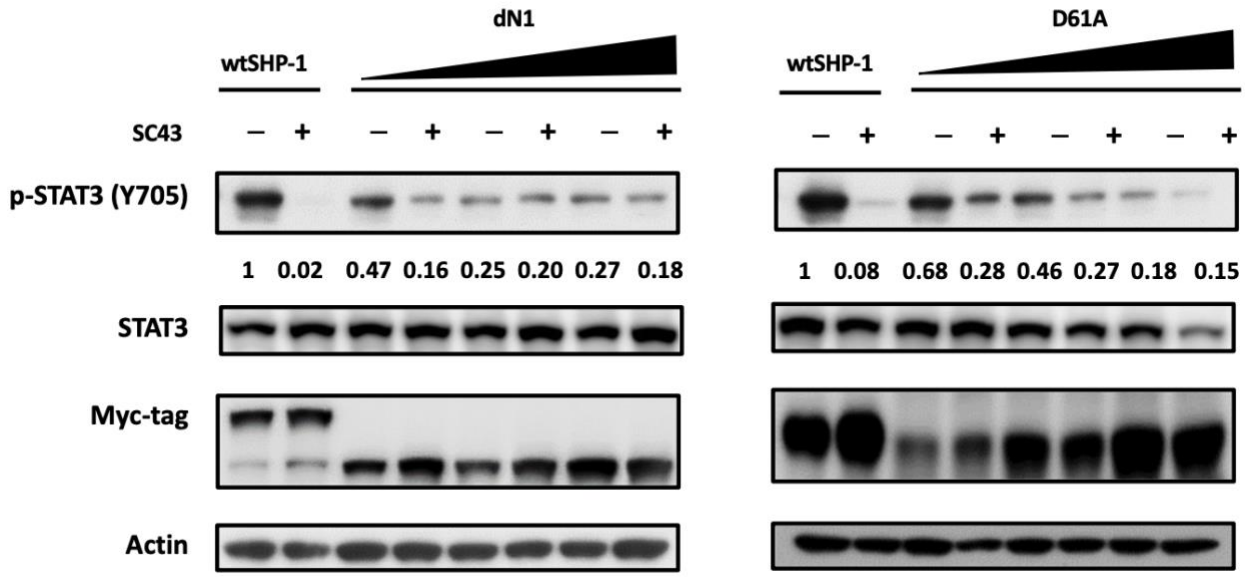

Figure 9. Dose-escalation study of transfection of dN1 and D61A on p-STAT3. Dose-dependent dN1 (left) and D61A (right) plasmid transfection suppressed p-STAT3 expression and decreased SC-43-induced p-STAT3 downregulation.

doi:10.6342/NTU202404281

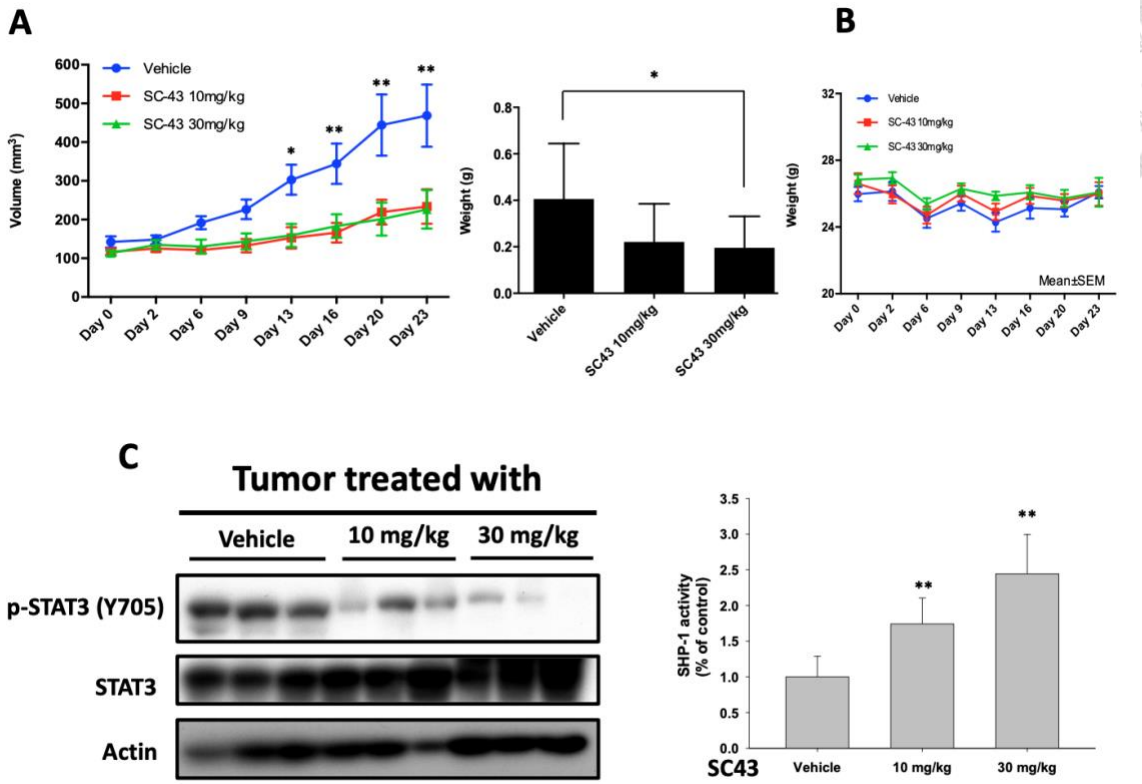

Figure 10. *In vivo* effects of SC-43 in CCA xenograft animal model. A. SC-43 exhibited significant tumor growth inhibition in a HuCCT1-bearing CCA subcutaneous model. Left, mice received SC-43 at 10 mg/kg/day or 30 mg/kg/day and tumor growth was measured twice weekly. Point, means; bars, SE ($n \geq 9$). Right, tumor weight at the end of treatment. (*, $P < 0.05$; **, $P < 0.01$) B. Body weight of mice with SC-43 treatment. C. Analysis of p-STAT3 and STAT3 in HuCCT1 tumors (left). SHP-1 phosphatase activity in HuCCT-1 tumors (right). Columns, mean; bars, SD ($n \geq 6$). (**, $P < 0.01$)

doi:10.6342/NTU202404281

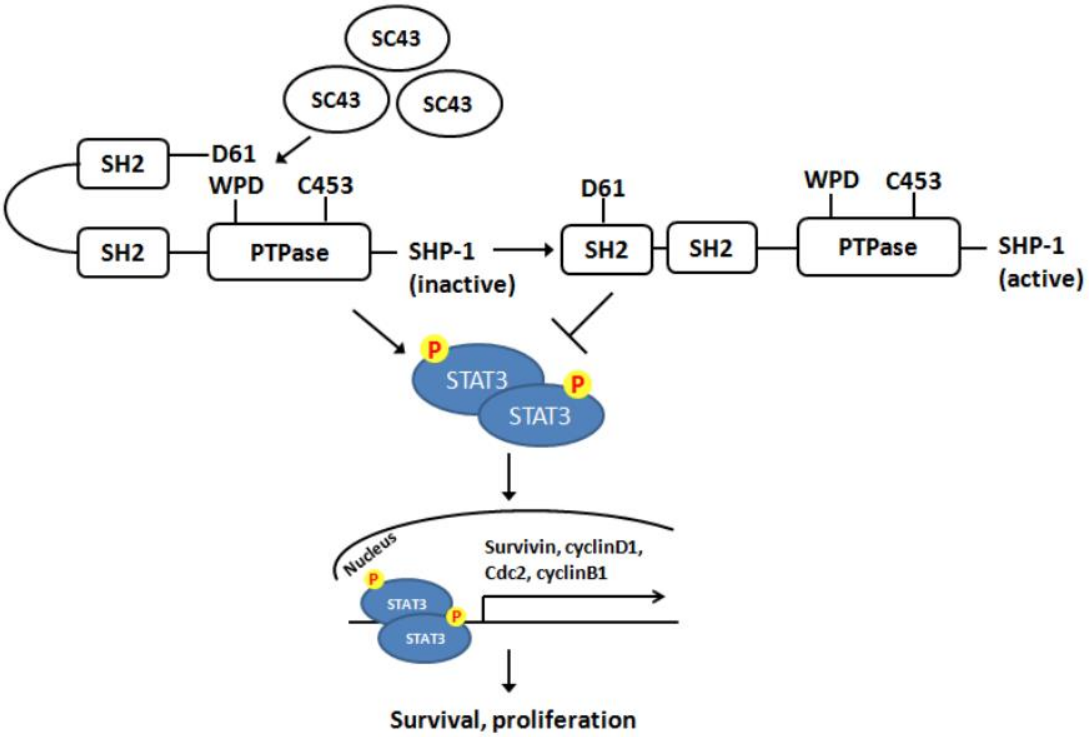

Figure 11. Summary model. SC-43 induced potent apoptosis in CCA by relieving the inhibitory N-SH2 domain of SHP-1 and downregulating p-STAT3, cyclin B1 and Cdc2.

doi:10.6342/NTU202404281

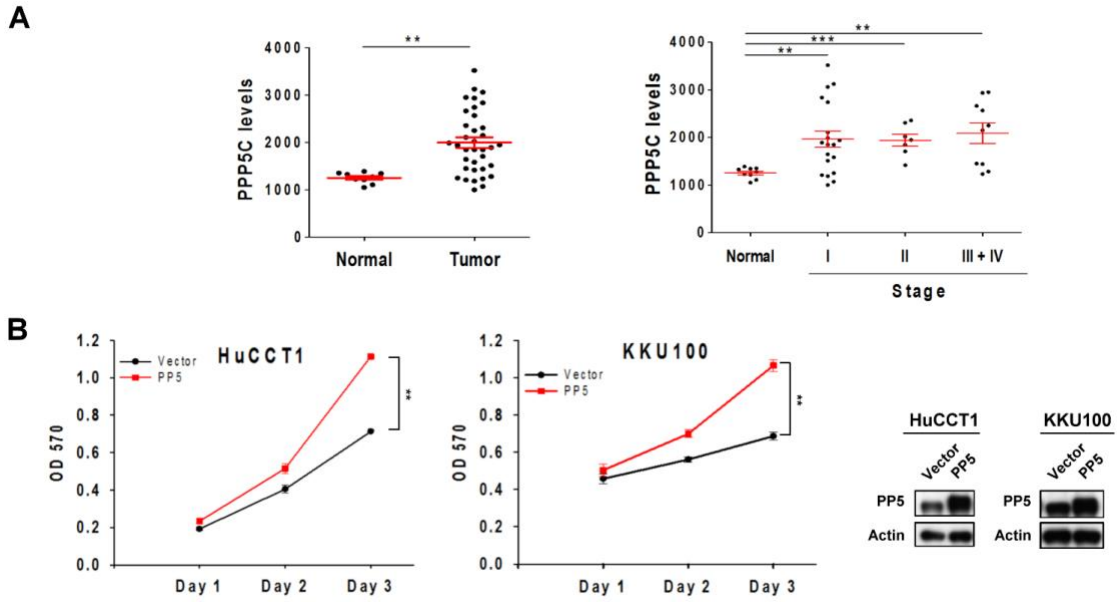

Figure 12. PP5 overexpression correlates with increased cell proliferation in CCA.

A. *PPP5C* expression data from normal tissue and CCA samples were downloaded from TCGA and the Broad GDAC Firehose data portal (left). Levels of *PPP5C* in tumor samples from CCA patients were then divided according to the stage classification (right). Levels of *PPP5C* in the CCA tumor tissues stages I to IV were compared with those of normal tissues. Data are shown as mean ± SE. (Normal tissues, n = 9; tumor tissues, n = 36; **, $P < 0.01$; ***, $P < 0.001$) B. PP5 overexpression induces cholangiocarcinoma cell proliferation. CCA cell proliferation was assessed by performing MTT assays. Data are shown as mean ± SD (n=8). (**, $P < 0.01$); the western blots in the right panel show overexpression of PP5 in KKU100 and HuCCT1 cells after lentiviral transfection of PP5.

doi:10.6342/NTU202404281

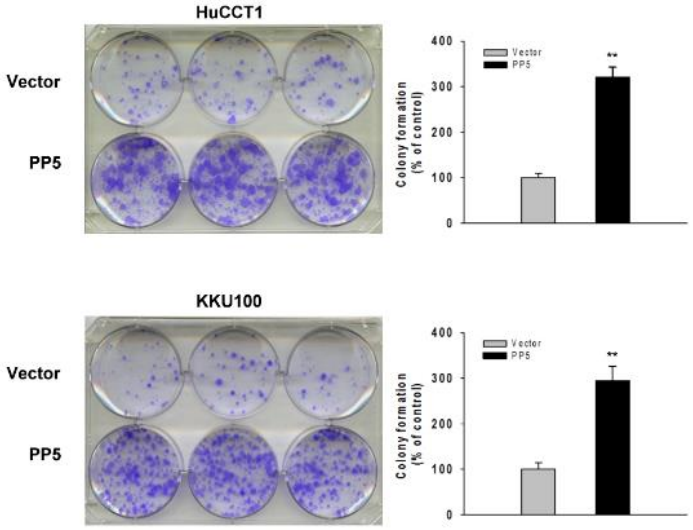

Figure 13. PP5 overexpression induce tumorigenicity in CCA. Colony formation assay were performed to evaluate the impact of PP5 overexpression on CCA cells. Values are shown as mean ± SD (n≥3). (**, $P < 0.01$)

doi:10.6342/NTU202404281

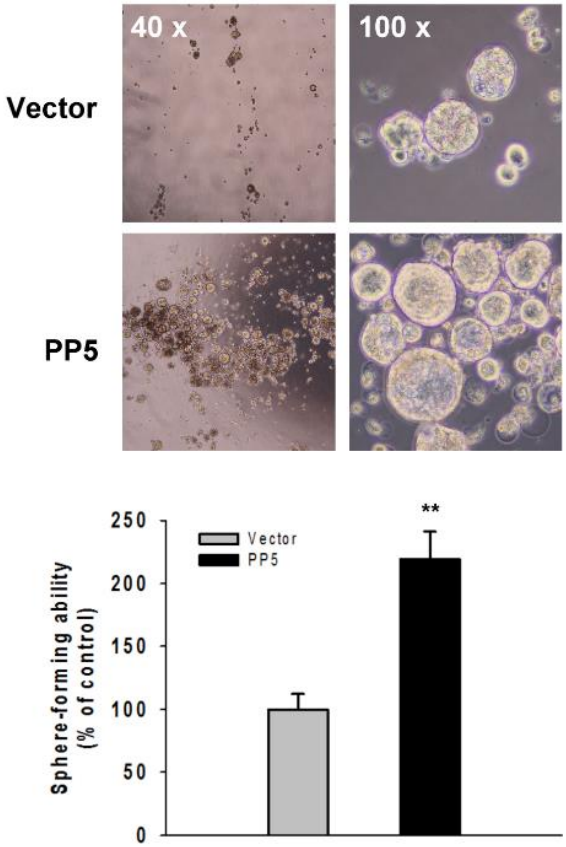

Figure 14. PP5 overexpression induce tumorsphere formation in CCA. Tumorsphere formation assay were performed to evaluate the impact of PP5 overexpression on CCA cells. Values are shown as mean ± SD (n≥3). (**, $P < 0.01$)

doi:10.6342/NTU202404281

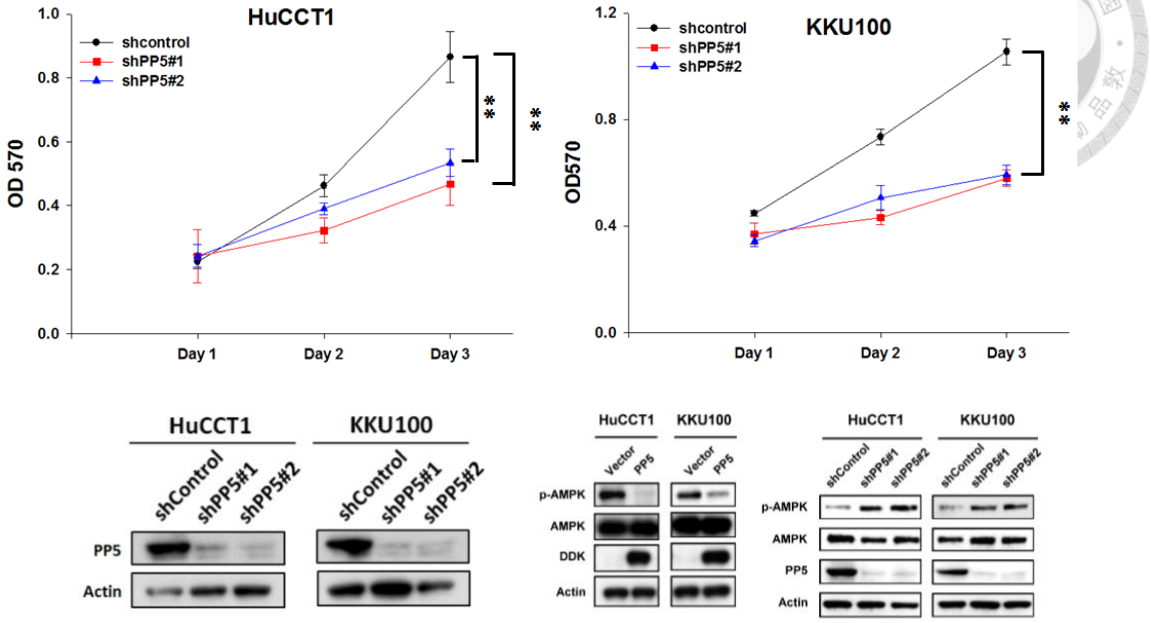

Figure 15. Knockdown of PP5 in CCA cells suppressed tumor growth. HuCCT1 and KKU100 cells were cultured at a density of 500 cells per well for 2 weeks to examine the effects of PP5 knockdown on CCA colony formation. Columns, mean; bars, SD (n=4). (**, $P < 0.01$) The western blots showed that p-AMPK was downregulated in PP5-overexpressing CCA cells, whereas p-AMPK was upregulated in PP5-knockdown cells.

doi:10.6342/NTU202404281

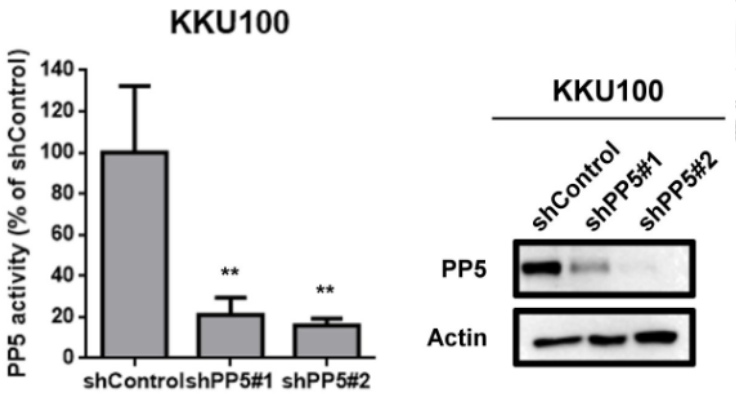

Figure 16. PP5 downregulation reduced PP5 activity in CCA cells. PP5 activity was measured in PP5-knockdowned CCA cells by using the RediPlate 96 EnzChek Serine/Threonine Phosphatase Assay Kit.

doi:10.6342/NTU202404281

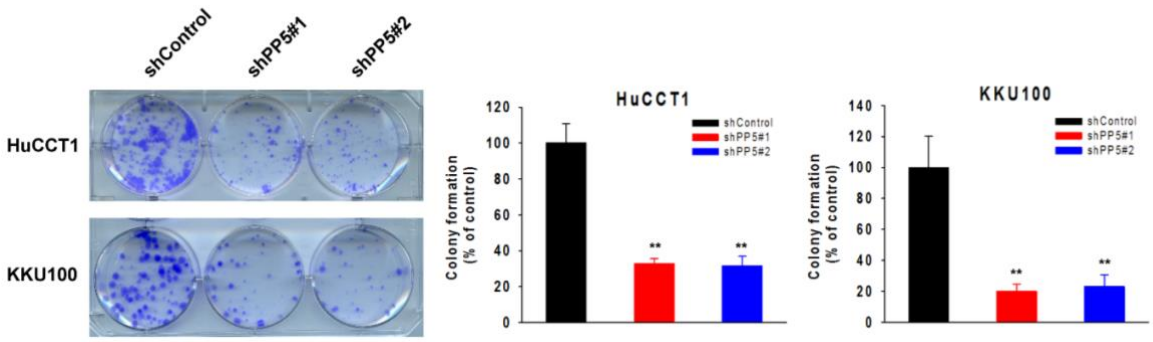

Figure 17. Knockdown of PP5 in CCA cells suppressed tumor growth. HuCCT1 and KKU100 cells were cultured at a density of 500 cells per well for 2 weeks to examine the effects of PP5 knockdown on CCA colony formation. Columns, mean; bars, SD (n=4). (**, $P < 0.01$)

doi:10.6342/NTU202404281

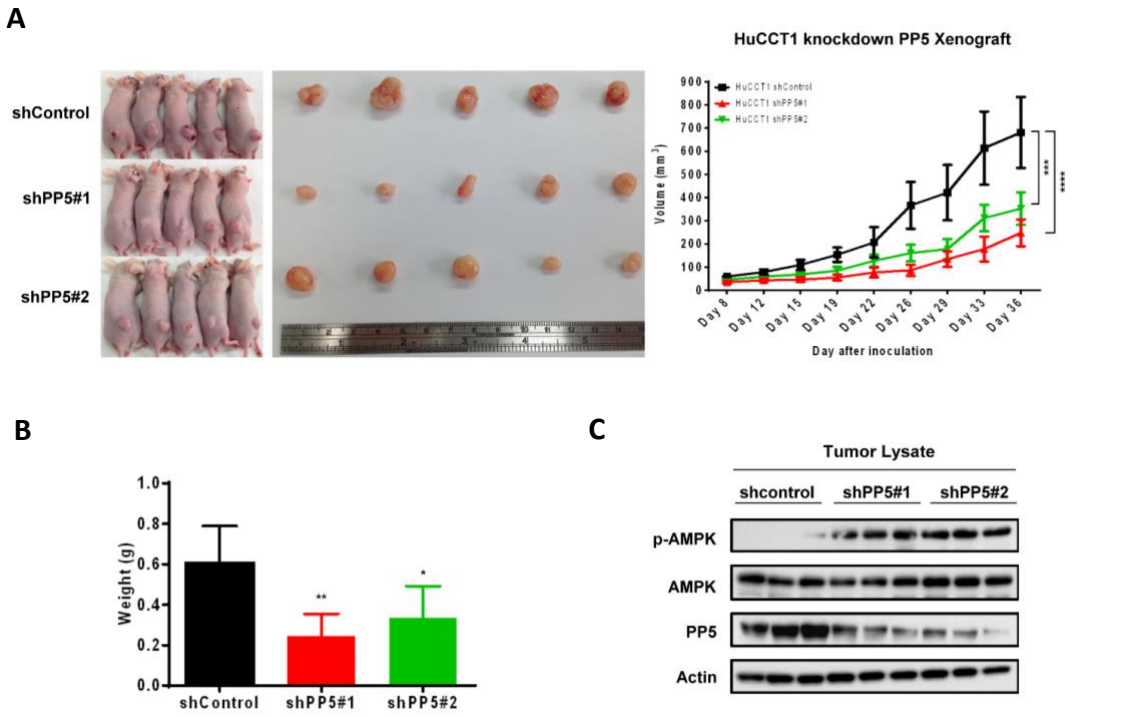

Figure 18. Knockdown of PP5 in CCA cells suppressed tumor growth. A. Image of tumors and the tumor growth curve of shPP5s-transduced HuCCT1-bearing mice. Values are shown as mean ± SEM (*n*=5). (***, $P < 0.001$) B. A histogram of tumor weight analysis. Values are shown as mean ± SEM (*n*=5). (*, $P < 0.05$; **, $P < 0.01$) C. Western blots using tumor lysates were performed to analyze the expression of p-AMPK and PP5.

doi:10.6342/NTU202404281

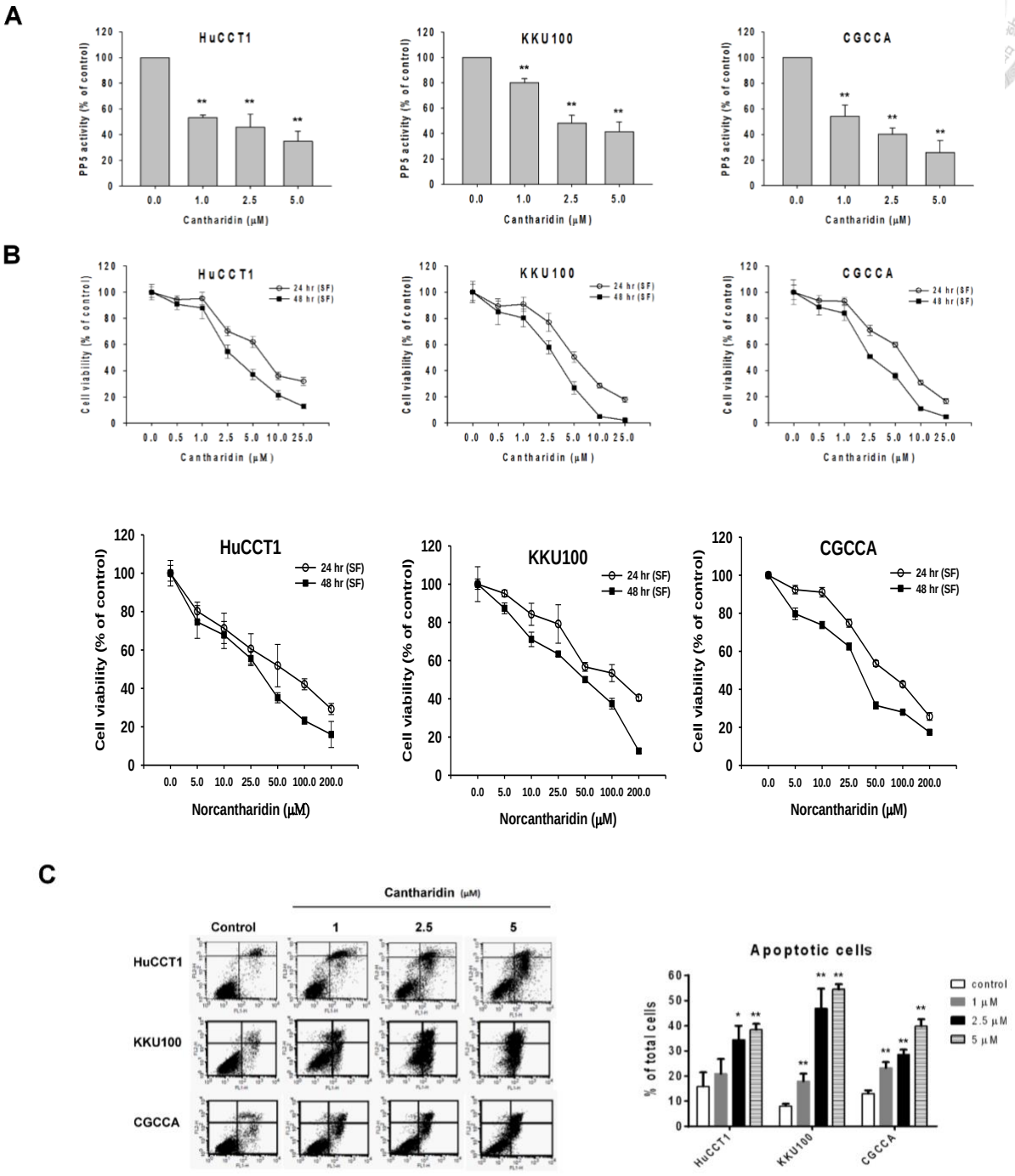

Figure 19. CTD inhibits CCA cell survival with p-AMPK upregulation. A. CTD treatment reduced PP5 activity in CCA cells. Data are shown as mean ± SD (*n*=3). (**, $P < 0.01$) B. MTT assays showed that CTD and NCTD treatment led to decreased cell viability in CCA cells. Data are shown as mean ± SD (*n*=8). C. The percentage of apoptotic CCA cells after CTD treatment for 24

doi:10.6342/NTU202404281

hours was examined using Annexin-V/propidium iodide staining followed by flow cytometry analyses. Data are shown as mean ± SD (n=3). (*, $P < 0.05$; **, $P < 0.01$)

doi:10.6342/NTU202404281

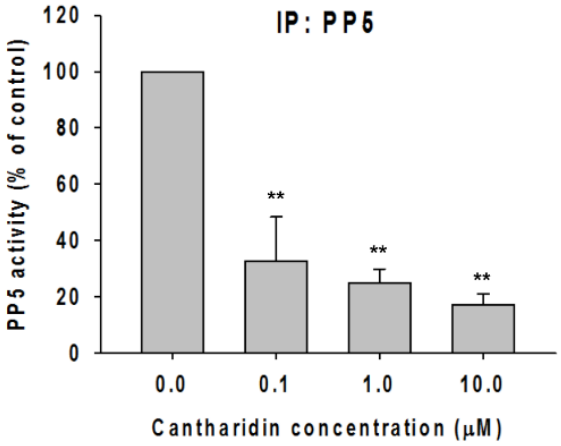

Figure 20. CTD reduced PP5 activity. Treating PP5-containing immunoprecipitant with CTD at indicated concentration in cell-free settings reduce PP5 activity (*n*=3). (**, $P < 0.01$)

doi:10.6342/NTU202404281

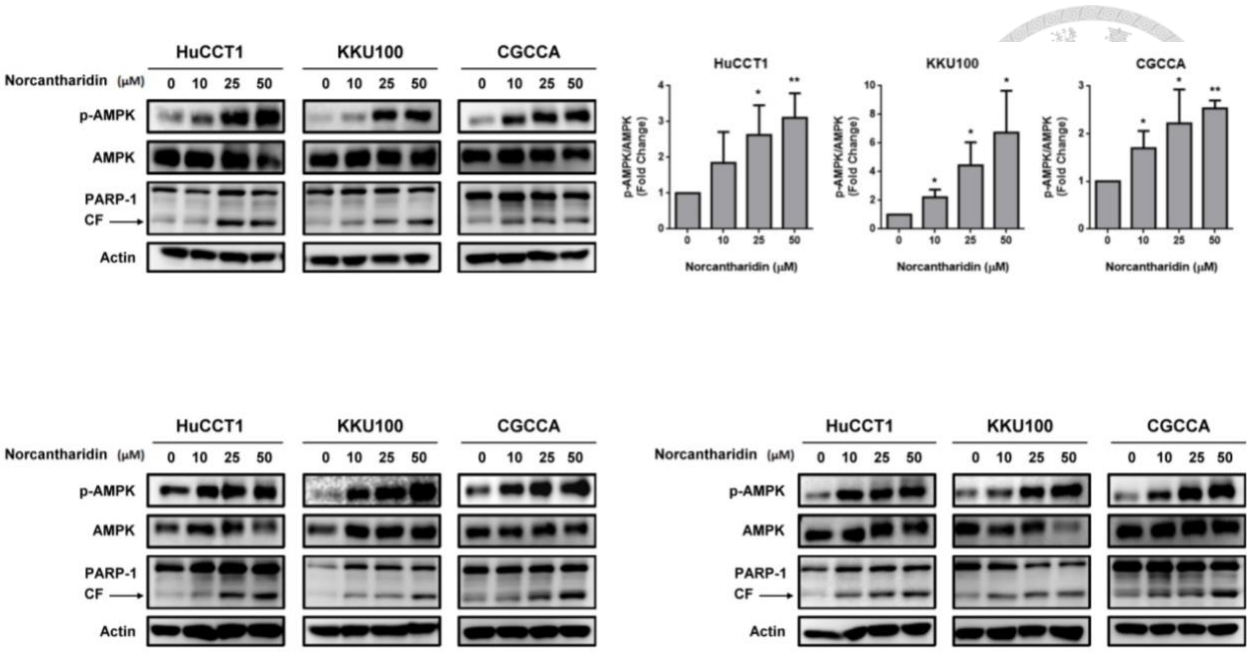

Figure 21. NCTD upregulated p-AMPK. NCTD treatment induced a dose-dependent p-AMPK enhancement in CCA cells (*n*=3). (*, $P < 0.05$; **, $P < 0.01$)

doi:10.6342/NTU202404281

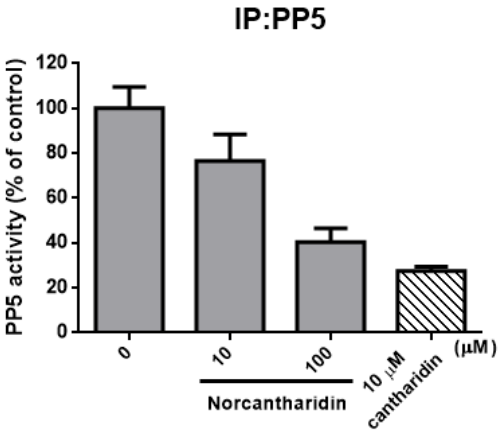

Figure 22. NCTD decreased PP5 activity. Treating PP5-containing immunoprecipitant with NCTD at indicated concentration in cell-free settings reduce PP5 activity (*n*=3).

doi:10.6342/NTU202404281

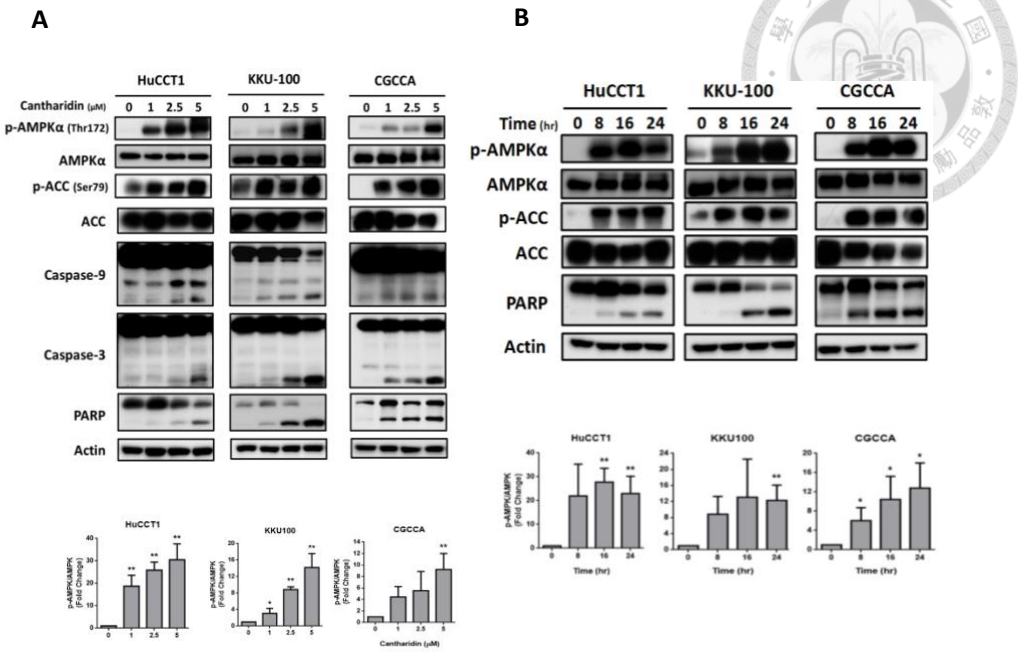

Figure 23. CTD inhibits CCA cell survival with p-AMPK upregulation. A. Representative western blot images showing that p-AMPK, p-ACC, cleaved Caspase-9, Caspase-3, and PARP-1 increased in a dose-dependent manner in response to CTD treatment. B. The expression of p-AMPK, p-ACC and the cleavage form of PARP-1 at different time points under 5 μM of CTD.

doi:10.6342/NTU202404281

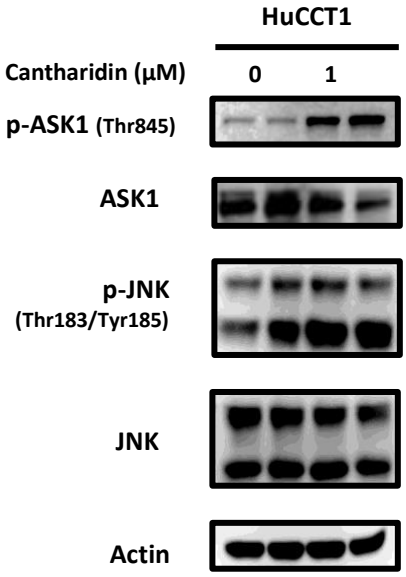

Figure 24. CTD upregulate p-ASK1 and p-JNK. Representative western blot images showing that p-ASK1 and p-JNK increased in response to CTD treatment.

doi:10.6342/NTU202404281

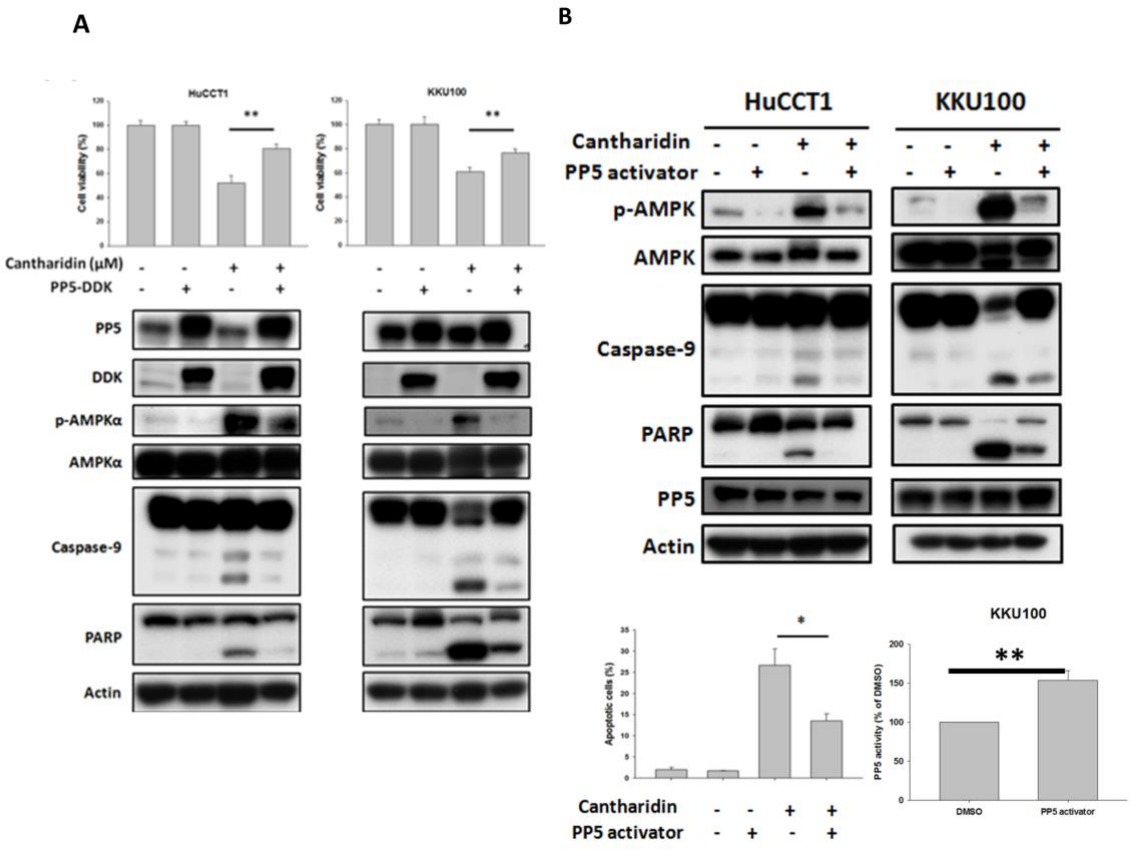

Figure 25. The PP5-AMPK signaling cascades play a critical role regulating CCA cell survival. A. PP5 overexpression rescued cell death induced by CTD. Cells ectopically expressing PP5-DDK were treated with 2.5 μM CTD before being collected for MTT assays and western blotting. The results of the MTT assays were quantified. Columns, mean; bars, SD (n = 8). (**, P < 0.01) B. Enhancing PP5 activity alleviated CTD-associated apoptosis in CCA cells. CCA cells were treated with 50 μM arachidonic acid for 3 hours followed by 2.5 μM CTD for 24 hours. The cells were then harvested for western blotting and apoptosis analyses. Columns, mean; bars, SD (n = 3). (**, P < 0.01)

doi:10.6342/NTU202404281

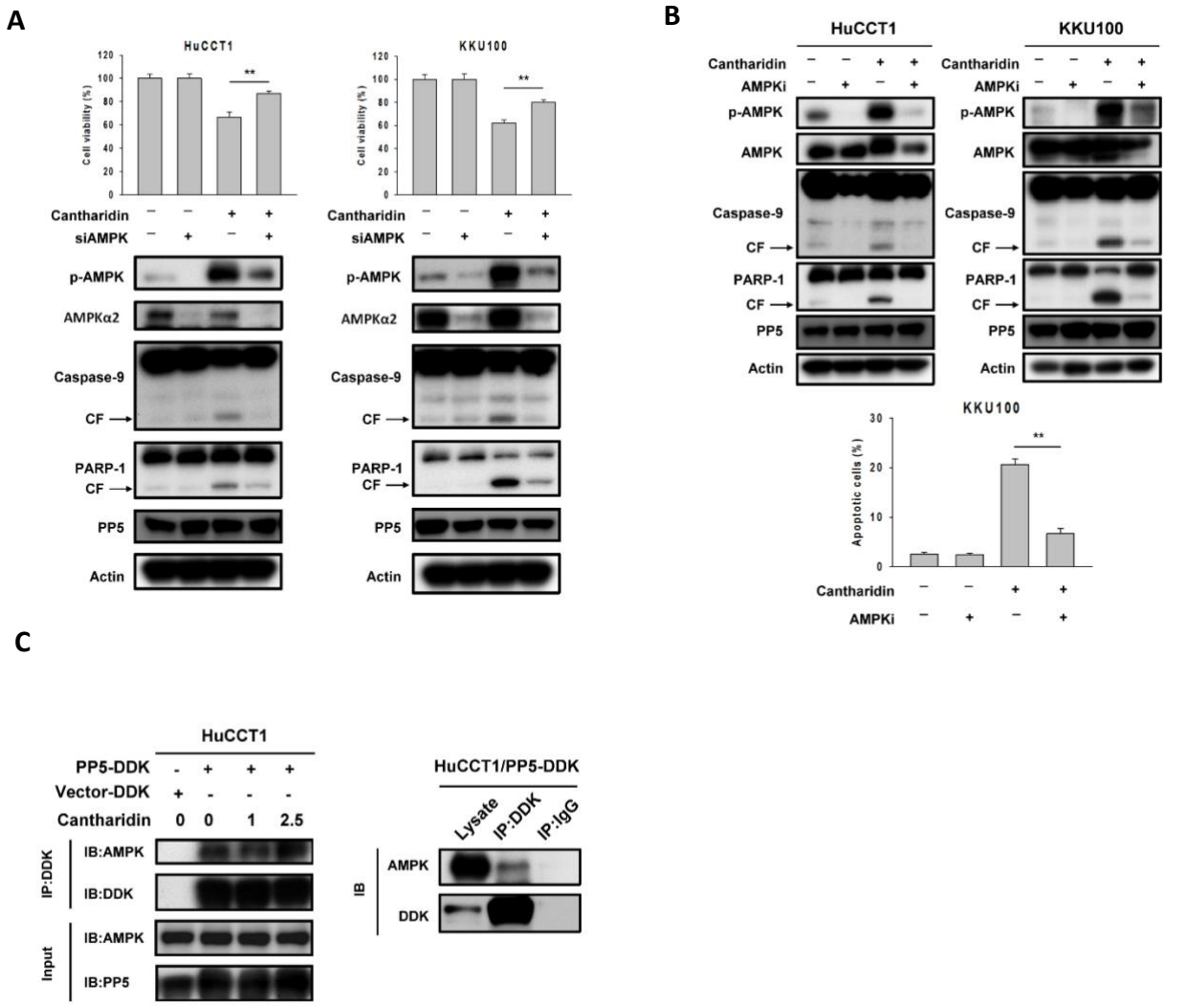

Figure 26. The PP5-AMPK signaling cascades play a critical role regulating CCA cell survival. A. CCA cells were transfected with siRNA against AMPK before being treated with 2.5 μM of CTD for 24 hours, then MTT assays and western blots were performed. Columns, mean; bars, SD (*n*=8). (**, $P < 0.01$) B. Cells were treated with 5 μM of dorsomorphin dihydrochloride (compound C) for 3 hours to inhibit AMPK activity. Next, 2.5 μM of CTD was applied for 24 hours. Cells were then collected for apoptotic assays and western blots. Columns, mean; bars, SD (*n*=3). (**, $P < 0.01$) C. HuCCT1 cells ectopically expressing PP5-DDK or control vector were treated with CTD before being immunoprecipitated with antibodies against DDK. Immunoprecipitants were collected for western blot analyses.

doi:10.6342/NTU202404281

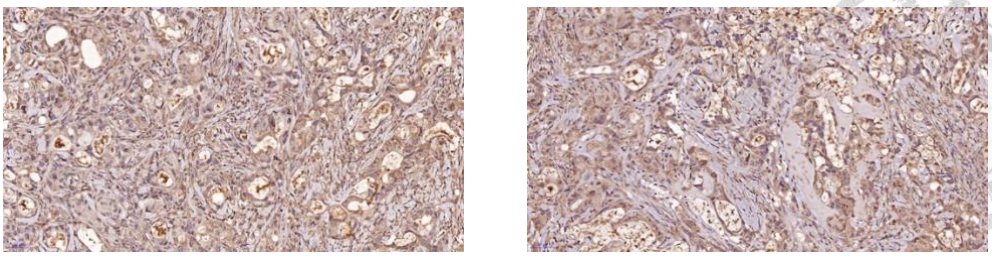

Figure 27. PP5 IHC after NCTD treatment. PP5 IHC revealed decreased level in NCTD-treated tumor.

doi:10.6342/NTU202404281

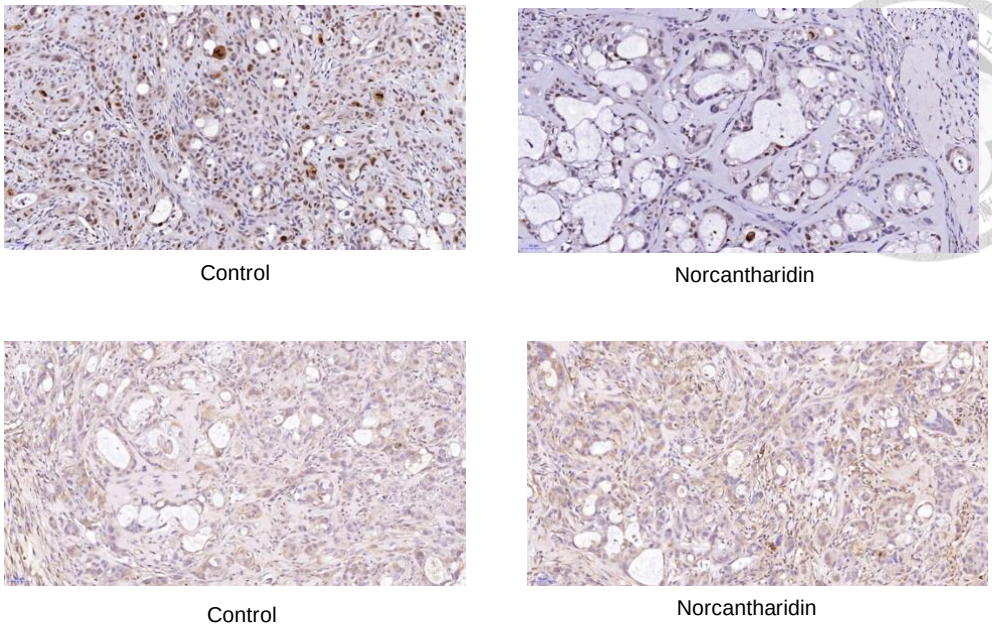

Figure 28. NCTD "*in vivo*" effect on Ki67 and TUNEL expression. NCTD-treated tumor revealed decreased Ki67 expression (upper). In contrast, NCTD treatment induced elevated TUNEL expression (lower).

doi:10.6342/NTU202404281

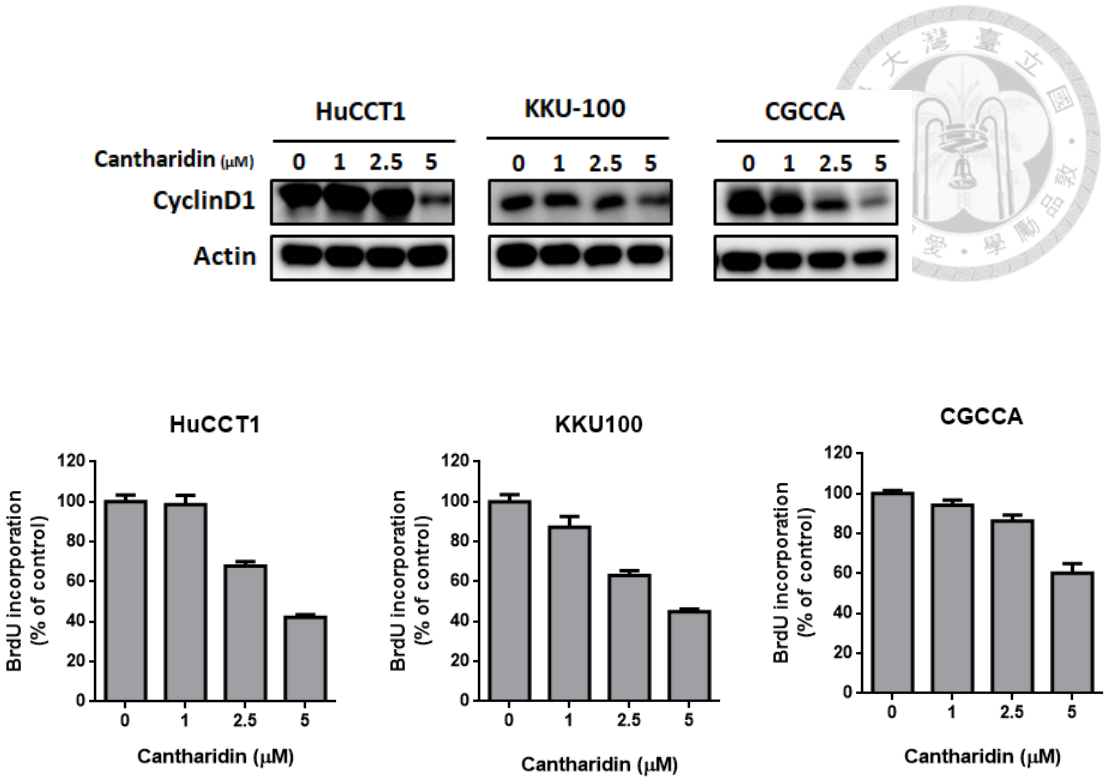

Figure 29. CTD downregulate Cyclin D1 and BrdU. CTD downregulate proliferative marker such as Cyclin D1(upper) and BrdU (lower) in CCA cells.

doi:10.6342/NTU202404281

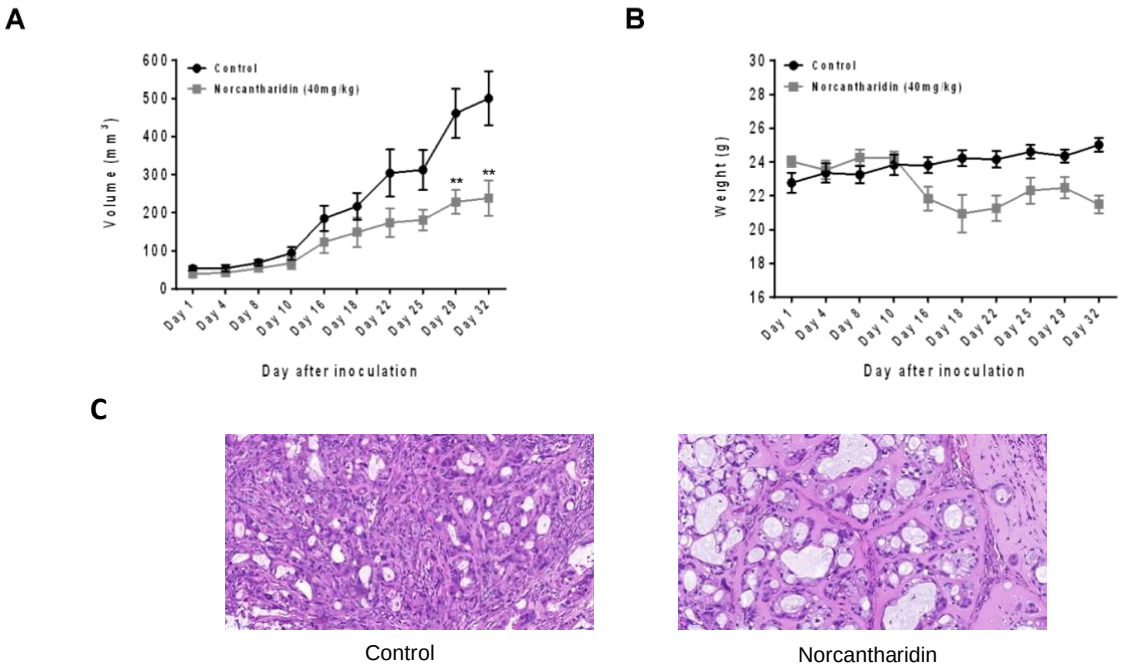

Figure 30. Pharmacologic inhibition of PP5 represses CCA tumor growth *in vivo*. A. The tumor growth curve of HuCCT1-bearing mice treated with NCTD (40 mg/kg) or vehicle control ($n \geq 3$ in each group) (*, $P < 0.05$; **, $P < 0.01$) B. The body weight of HuCCT1-bearing mice ($n \geq 3$ in each group). C. H&E stain from xenograft tumor after NCTD treatment.

doi:10.6342/NTU202404281

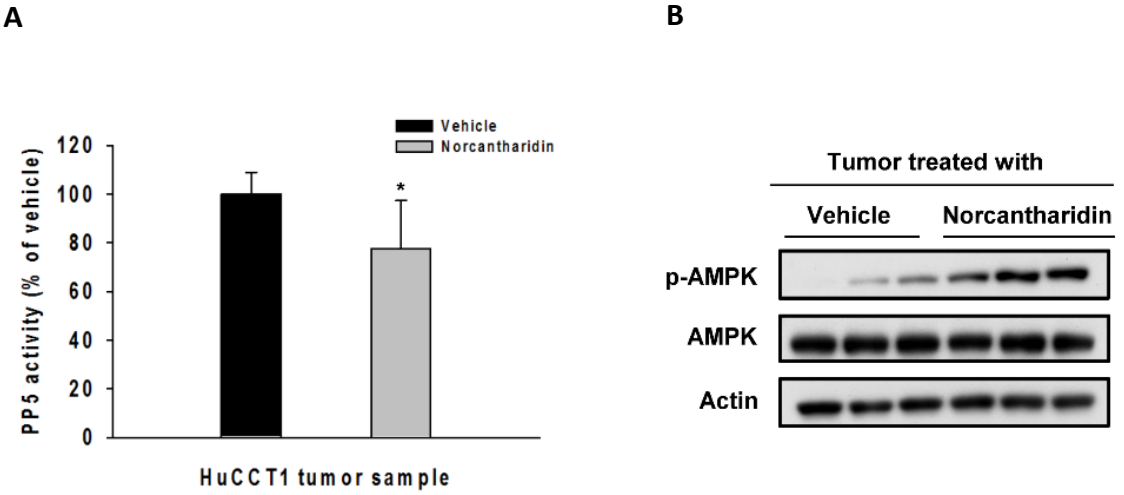

Figure 31. Pharmacologic inhibition of PP5 represses CCA tumor growth *in vivo*. A. The PP5 activity of tumor samples from NCTD or vehicle-treated mice ($n \geq 3$ in each group) (*, $P < 0.05$) B. The expression of p-AMPK in tumor samples ($n=3$ in each group).

doi:10.6342/NTU202404281

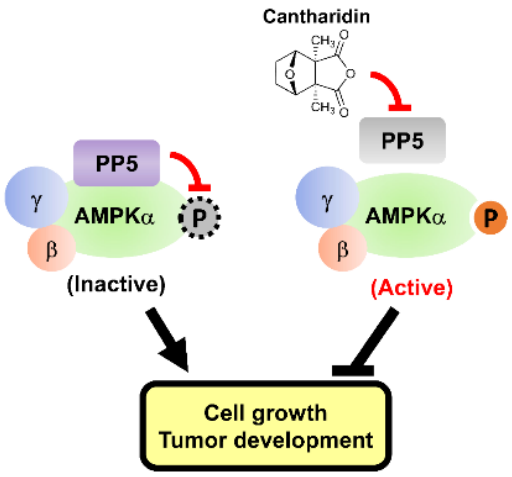

Figure 32. Visual abstract of pharmacologic inhibition of PP5 in treating CCA tumor growth *in vivo*. PP5 dephosphorylates AMPK to promote CCA cancer development. PP5 induces CCA cell growth and tumor progression though dephosphorylation of AMPK (inactivation). PP5 inhibitor CTD suppressed tumor growth by increased p-AMPK.

doi:10.6342/NTU202404281

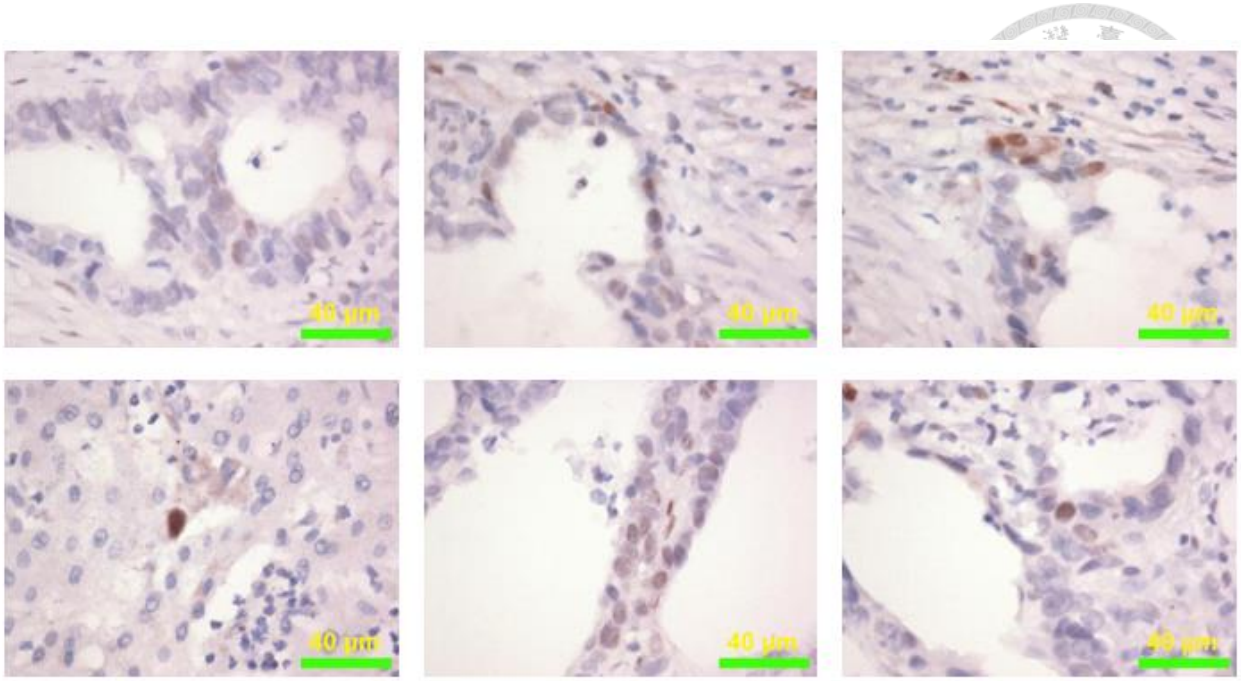

Figure 33. Immunohistochemical (IHC) staining for p-STAT3 in CCA tumor. Examples of weak-staining p-STAT3 in our human CCA specimen.

doi:10.6342/NTU202404281